

Records of Geomagnetic Reversals From Volcanic Islands of French Polynesia

2. Paleomagnetic Study of a Flow Sequence (1.2-0.6 Ma) From the Island of Tahiti and Discussion of Reversal Models

ANNICK CHAUVIN AND PIERRICK ROPERCH^{1,2}

ORSTOM et Laboratoire de Géophysique Interne, Université de Rennes 1, Rennes, France

ROBERT A. DUNCAN

College of Oceanography, Oregon State University, Corvallis

A volcanic sequence almost 700 meters thick has been sampled in the Punaruu valley on the island of Tahiti, southern central Pacific Ocean. Detailed paleomagnetic results have been obtained from 123 sites. Three reversals are recorded in this sequence. Age determinations (K-Ar) indicate that the youngest reversal corresponds to the Matuyama-Brunhes transition while the two other transitions limit the Jaramillo normal polarity subchron. An apparent R-T-R excursion has been identified lower in the volcanic sequence and K-Ar age determinations around 1.1 Ma suggest that it corresponds to the Cobb Mountain subchron, but no normal paleomagnetic directions were discovered. The Matuyama-Brunhes and the lower Jaramillo transition are defined by only a few intermediate directions while many intermediate directions are observed for the upper Jaramillo transition and the Cobb Mountain excursion. We attribute these differences to variations in the rate of eruption of the volcanic rocks. The lower Jaramillo record is characterized by a steepening of the inclination at the beginning of the reversal suggesting a possible axisymmetric control of the field at this stage. However, the transition path for the most detailed record (upper Jaramillo) is characterized by large loops; this prevents simple modeling of the transition by low order zonal harmonics at all stages of a reversal. Paleointensity determinations were attempted on 48 samples with reliable results obtained for 26 of them. Paleointensities for the transitional field range from 3 to 8 μ T. Such very low field strengths were first suggested by the low intensity of the natural remanent magnetization associated with intermediate directions. An analysis of the variation of the intensity of magnetization with the angular departure from the central axial field, including all other available data from Polynesia, indicates that (1) a paleomagnetic direction should be considered as intermediate when it is more than 30° from the expected axial dipole direction, and (2) the average transitional geomagnetic field intensity is about 1/5 of its value during stable polarity states. Comparison of these results observed in Polynesia with previous studies from Iceland suggests an increase of the average intensity of the intermediate field with latitude.

INTRODUCTION

The study of the secular variation of the Earth's magnetic field [Le Mouél, 1984; Gire et al., 1986; Gubbins, 1987; Bloxham, 1988] has provided some insight, even if sometimes controversial, on fluid motion in the Earth's core, leading to a better understanding of the geomagnetic dynamo. Paleomagnetic studies of the behavior of the geomagnetic field during polarity transitions constitute another important way to constrain the various models of the origin of the Earth's magnetic field. In this paper, we will focus on the second approach in reporting some new data on reversals recorded by a sequence of volcanic flows from the island of Tahiti (French Polynesia).

Since the beginning of the study of reversals [Sigurgeirsson, 1957; Van Zijl et al., 1962] a great number of paleomagnetic records of transitions have been obtained. The first major step was to recognize the non-dipole character of the transitional field [Dagley and Lawley, 1974; Hillhouse and Cox, 1976]. Because the transitional path lay in a restricted sector of longitude, Hillhouse and Cox [1976] suggested that reversals recorded at one site might be controlled by a standing non-dipole field. Models with axial

symmetry were then proposed by Hoffman [1977] and Hoffman and Fuller [1978]. However, evidence for non-axisymmetric components led to 'flooding' models which included both north-south and east-west components [Hoffman, 1979, 1981a]. Similar approaches, using low order Gauss coefficients, were proposed by Williams and Fuller [1981]. Such models have been under active consideration by paleomagnetists because they have provided a guideline for the analysis of records of the intermediate field. However, in order to determine the morphology of the transitional field, more numerous paleomagnetic records with better resolution are required. In particular, widely-spaced, multiple records of individual reversals and successive reversals at the same site are necessary. The last polarity transitions (the Matuyama-Brunhes and the boundaries of the Jaramillo and Olduvai events) are already the best documented; adding new records of these transitions will provide detailed understanding and constrain modeling of the behavior of the transitional field.

Since Hoffman [1979] showed the necessity for additional data from the southern hemisphere, several records have been obtained from southern low latitudes [Clement and Kent, 1984; Clement and Kent, 1985; Hoffman, 1986] as well as from the northern hemisphere [Clement and Kent, 1986; Liddicoat, 1982; Theyer et al., 1985; Herrero-Bervera, 1987; Valet et al., 1988b]. However, most of these data come from sedimentary rocks and several authors [Hoffman and Slade, 1986; Prévot et al., 1985b] have questioned the reliability of such records, particularly when they have low sedimentation rates. In a recent study of the Matuyama-Brunhes reversal recorded at Lake Tecopa, Valet et al. [1988a] have shown that a strong overprint from the following normal polarity

¹ Also at College of Oceanography, Oregon State University, Corvallis

² Permanently at Institut Français de Recherche Scientifique pour le Développement en Coopération, ORSTOM, Paris, France

Copyright 1990 by the American Geophysical Union

Paper number 89JB03452
0148-0227/90/89JB-03452\$05.00

period was not removed in the early study of *Hillhouse and Cox* [1976]. Because few studies have used thermal demagnetizations [Valet et al., 1988a,b; Laj et al., 1988], the extent of overprinting in the other available records is uncertain.

Only relative changes in paleointensity can be obtained from sedimentary rocks. The variations of the magnetic properties in the sediments are generally recognized through the variations of an artificial remanence, such as an isothermal or an anhysteretic remanent magnetization, but this method assumes that the NRM is not altered by a multicomponent magnetization. The normalization technique is also useless if geochemical alterations have occurred during diagenetic processes [Karlin and Levi, 1985]. Most estimates of the time duration of reversals come from sedimentary sections. Because several studies have shown a significant decrease in intensity before any changes in directions, the estimates vary from a few thousand years to several thousand years, depending on how the transition boundaries are defined.

While sediments provide only average field directions and relative paleointensity changes in the best cases, volcanic rocks generally enable a well-determined paleofield direction and sometimes accurate determinations of the absolute paleointensity. However, with volcanic records of reversals, the time resolution of the transition is generally not well established due to a poor knowledge of the rate of extrusion of the lava flows.

A common feature in all records is a significant decrease in the paleointensity of the field during transitions, but up to now most studies have focussed on the directional behavior during reversals rather than analyzing the field as a complete vector. When paleointensity data are added to the directional records, some unexpected characteristics of the intermediate field appear, which are not shown by directional data alone. The most complete description of the behavior of the geomagnetic field, in direction and intensity, comes from the study of the volcanic record of a Miocene age reverse to normal transition on the Steens Mountains of SE Oregon [Mankinen et al., 1985; Prévot et al., 1985a]. Very rapid field variations (a few thousand gammas per year) have been suggested by Coe and Prévot [1989], but have not yet been fully established. Apart from the large decrease in intensity during transition, which is the main characteristic, Shaw [1975, 1977] has also suggested that the intermediate field may occasionally reach some high intensity values. On the other hand, large variations in paleointensity without changes in direction were shown by Shaw [1977] and by Prévot et al. [1985b]. We will discuss why some paleointensities may not be valid due to several experimental problems.

Volcanic rocks provide reliable and precise spot-readings of the paleomagnetic field but it is not easy to obtain a sequence that has recorded a detailed polarity reversal; generally only partial records are found [Bogue and Coe, 1984]. In this paper, we report paleomagnetic results obtained from a volcanic sequence almost 700 meters thick on the island of Tahiti (French Polynesia, south central Pacific Ocean). Within this section, four transitional zones have been found and two of them have recorded various intermediate directions.

GEOLOGICAL SETTING

The Society archipelago, in the southern central Pacific Ocean, is composed of volcanic islands which are aligned in a WNW-ESE direction delineating the Pacific plate motion during the last 5 m.y. [Duncan and McDougall, 1976]. The island of Tahiti is the largest of the Society Islands and is made of two coalesced volcanos (Tahiti Nui and Tahiti Iti). The Tahiti Nui volcano is a cone rising 6000 meters above the surrounding abyssal seafloor, of

which only one-third is subaerial. The erosion of the island has carved radial valleys which enable the sampling of volcanic sequences. A few transitional paleomagnetic directions were first reported by one of us [Duncan, 1975] in the Punaruu valley, which is one of the deepest valleys of Tahiti Nui (Figure 1a). This discovery suggested that some volcanic activity occurred at reversal boundaries and that this volcanic sequence might provide detailed behavior of the transitional field.

GEOLOGY AND GEOCHRONOLOGY OF VOLCANIC ROCKS FROM THE PUNARUU VALLEY

The thick succession of seaward-dipping lava flows exposed in the Punaruu Valley was erupted during the main phase of shield construction at the Tahiti Nui volcano. These are typically blocky 'aa' flows with rubbly oxidized top surfaces and massive interiors, easily traced for hundreds of meters along the canyon walls. The thickness of the flows varies between 1 and 4 m, with a mean of 3 m. Rapid erosion during periodic storms and active quarrying have exposed fresh outcrop surfaces. Compositionally these rocks are alkali basalts, but range considerably in phenocryst content from porphyritic (picrites and ankaramites) to aphyric varieties. Samples with T74 prefixes have been described by Duncan [1975]. Complete geochemical and mineralogical analyses of the dated samples will be reported elsewhere.

Samples selected for K-Ar dating were first examined in thin section to determine the state of alteration of the K-bearing phases. In most cases the rocks are petrographically fresh and well-crystallized. Samples which showed patchy groundmass alteration to clays or glassy mesostasis were excluded. Samples bearing cumulate olivine and rare small peridotite xenoliths were also eliminated because of the possibility of mantle-derived argon carried in xenocrysts.

After removal of any weathered surfaces, each sample was crushed to chips (0.5 to 1.0 mm size) and ultrasonically cleaned in distilled water. A representative split of this fraction was powdered and K-concentration was determined by atomic absorption spectrophotometric methods. Argon was extracted from the coarse chips by radio-frequency inductive heating in a high vacuum glass line equipped with ^{38}Ar spike pipette and Ti-TiO₂ getters for removing active gases. The isotopic composition of argon was then measured mass spectrometrically using a model AEI MS-10S instrument with computer-controlled peak selection and digital data acquisition and reduction.

The age determinations on 12 samples from the Punaruu valley section appear in Table 1. The positions of these dated samples are shown in Figure 1b. With the exception of the age of sample T85-76 which appears to be slightly too young, the age succession is consistent with the stratigraphic order of the lava flows. The ages and magnetic polarities of the rocks are also compatible with the late Matuyama to early Brunhes portion of the magnetostratigraphic timescale (see later discussion of paleomagnetic transitions). This 700 m thick section was erupted between 1.2 and 0.6 Ma, yielding an average accumulation rate of 1.2 km per million years, or approximately one flow every two thousand years. The evidence from the paleomagnetic studies, however, indicates that flows were erupted in pulses with significant time gaps, rather than at regular intervals.

PALEOMAGNETIC SAMPLING

All the paleomagnetic sampling has been done within the Punaruu valley and was carried out during two field trips. The first one was a preliminary sampling during which 150 cores from 25 lava flows were collected. Preliminary results, associated with the

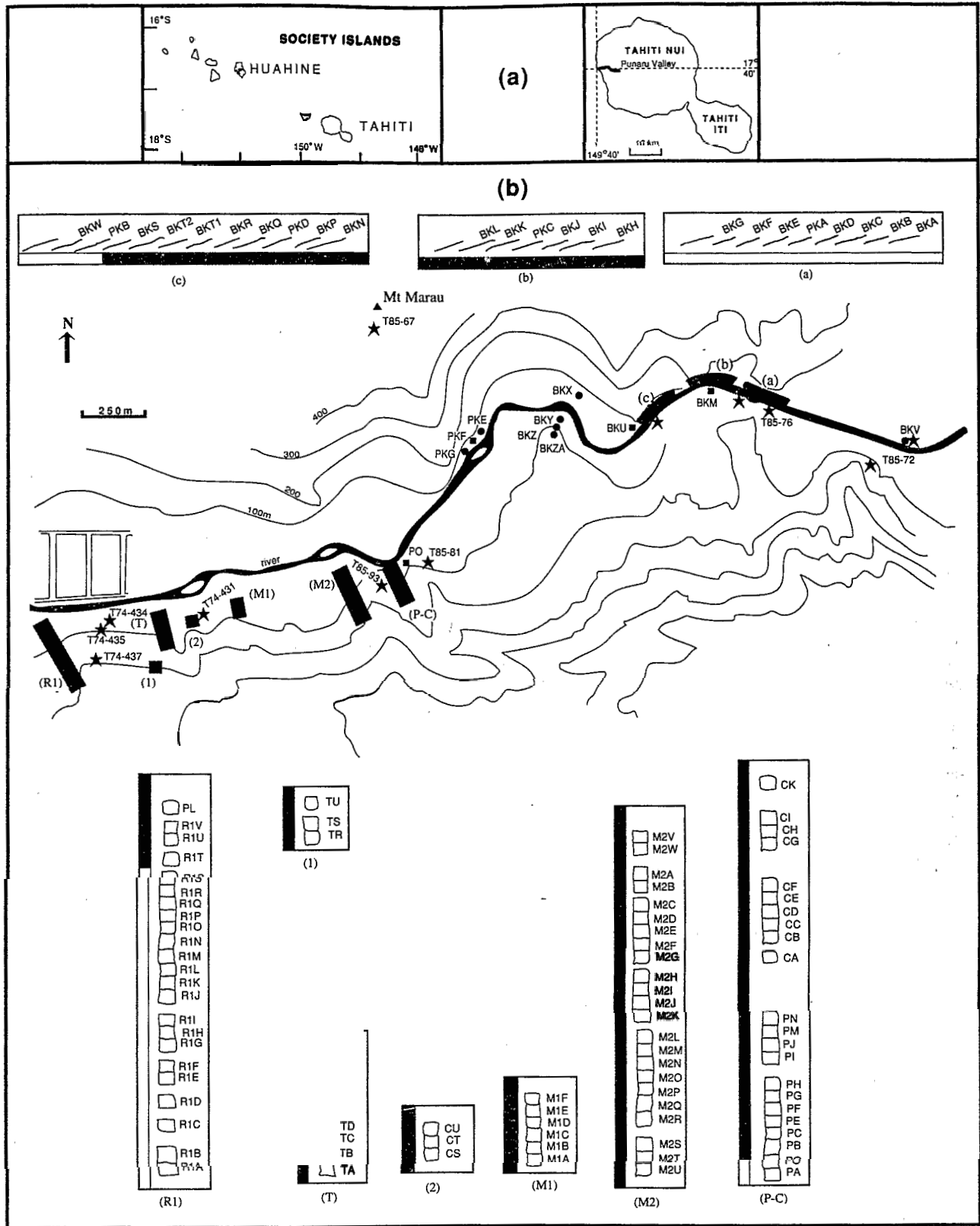


Fig. 1. a) Map of the Society islands (French Polynesia, south-central Pacific Ocean). The paleomagnetic sampling has been done along the Punaruu Valley in the western part of the island of Tahiti (b). Flows are dipping toward the west. On the north side of the valley, the sampling was done along the river as indicated by the 3 sections a, b, c. Filled circles correspond to flows below (site BKV) and above sections a, b, c. Squares are the sampling sites of the dikes. On the southern border of the river, numerous cross sections of the hillside have been done and are indicated by letters referenced in the text. The magnetic polarity (black for normal) has been shown within each section. Gaps in the sampling are also indicated by discontinuities within each section. Stars correspond to the location of the dated samples.

TABLE 1. K-Ar Age Determinations for Basalts from the Punaruu Valley, Tahiti

Sample Number	%K	Radiogenic $^{40}\text{Ar/g}$ ($\times 10^{-7}\text{cc}$)	%Radiogenic ^{40}Ar	Age $\pm 1\sigma$ (Ma)
BKV-185	0.83	1.7156	27.9	1.19 \pm 0.02
T85-72	0.86	1.5745	15.2	1.08 \pm 0.02
T85-76	1.03	1.7688	10.8	1.01 \pm 0.05
BKG-85	2.07	3.9120	24.4	1.09 \pm 0.02
PKB-14	1.16	2.2268	18.4	1.11 \pm 0.03
T85-81	1.03	1.8259	24.4	1.05 \pm 0.02
T85-93	1.28	2.1740	19.8	1.00 \pm 0.02
T74-431	1.62	2.8538	17.0	1.04 \pm 0.02
T74-434	1.16	1.8886	11.8	0.96 \pm 0.02
T74-435	1.34	2.0978	17.8	0.92 \pm 0.02
T74-437	1.66	2.1991	14.2	0.78 \pm 0.01
T85-67	2.19	2.3630	6.6	0.62 \pm 0.02

Age calculations based on the following decay and abundance constants: $\lambda_e = 0.581 \times 10^{-10} \text{ yr}^{-1}$, $\lambda_\beta = 4.962 \times 10^{-10} \text{ yr}^{-1}$; $^{40}\text{K}/\text{K} = 1.167 \times 10^{-4}$ mole/mole.

Jaramillo termination and the Brunhes onset, were reported by *Roperch and Chauvin* [1987]. More detailed sampling during the second field trip covered a distance of 4 km into the valley. This sampling interval corresponds to a volcanic sequence almost 700 meters thick.

A total of 788 cores have been drilled from 123 lava flows and 4 dikes, with an average of 6 to 7 cores per volcanic unit. Cores were obtained with a gasoline-powered portable core drill, and then oriented using a magnetic compass and, whenever possible by sun orientation. We have distributed the samples throughout the flows, vertically and horizontally, to minimize risks of systematic deviation of the paleomagnetic directions due to local block disturbances; in many cases, the location of the samples was determined by accessibility. During the sampling we used a small field spinner magnetometer (LETI) in order to recognize the polarities of the flows and map the stratigraphy. The intensity of the natural remanent magnetization (NRM) was often better than the NRM direction in recognizing transitional zones. Because of viscous components from the present day field, some transitional flows showed directions close to a normal polarity but with very low magnetic intensity. This information obtained with a portable spinner magnetometer was more accurate than fluxgate measurements of oriented blocks but, obviously, was more time consuming.

The natural dip of the lava flows is close to 10 degrees toward the ocean. This fact allowed us to sample either along the river or by vertical sections (Figure 1). The first part of the sampling was done along the river. A lava flow (BKV) with a reversed direction was found at the base of the sequence. Between BKV and the next flow (BKA), no outcrop was found. From BKA to BKG, a reverse polarity was observed. Following this reverse succession, there was a small gap in the sampling of a few tens of meters, followed by a transitional zone which contained 16 lava flows (from BKH to BKT2), over a horizontal distance of 350 m. One dike (BKM) with a reversed direction cuts the transitional sequence and was sampled near flow BKL.

Immediately above BKT2, we found 3 lava flows (BKS, PKB, BKW) and one dike (BKU) with reverse polarity. No normal direction was observed in this part of the volcanic sequence. No outcrop was available for the next 250 m along the river and taking into account a slope of ten degrees, this corresponds to a vertical gap of almost 40 meters in the sequence.

Then 4 flows with reverse directions were sampled: BKX on the north side of the river and BKY, BKZ, BKZA on the south side in an old quarry where the stratigraphic order was easy to recognize. Two other reverse flows PKE and PKG were sampled about 300 m west of the previous location. The dike PKF which cuts these two flows has a normal polarity. The river sites from flow BKV to PKG correspond to the lower part of our sequence.

The second part of the sampling was made along the southern wall of the valley. We tried to sample all flows which could be observed in the field but it was necessary to do several small sections because of a lack of outcrops or because of topographic difficulties, like small waterfalls. There were no indications either in the geological, geochronological or paleomagnetic data for differences in stratigraphy between the two sides of the river. No faults have been observed in the valley and young valley-filling flows, found further interior, are absent here.

The section P-C (flows PA to PN and CA to CK) begins near the river, about 350 m away from the flow PKG. A reverse polarity was observed for the bottom two flows, and a transitional zone was recorded by the overlying flows (PB, PC, PE, PF). A small baked soil, 50 cm thick, was interbedded between flows PC and PE but we were unable to sample it. No such well defined soil was seen elsewhere in our sequence. As it does not mark the transition from full reverse to full normal, but is interbedded between two flows having a similar direction, this soil horizon is not an indicator of a large time gap between two flows, in contrast to what we expected. A normal polarity was found above the transition up to an elevation of 125 m (flows PG to PN and CA to CK).

Section M2 extends from an elevation of 30 m to 120 m above the sea level. From M2U to M2G only normal directions were observed. The top seven flows from M2E to M2V in this section have transitional directions. Section M1 is about 400 m west of section M2 and is composed of 6 flows (M1A to M1F) with intermediate directions. The particular paleomagnetic directions recorded by the flows from the sections M1 are very similar to that observed at flows CS, CT, CU (named section 2 on Figure 1) which are situated 100 m west of section M1.

Section T is close by and just above flows CS, CT, CU and starts at an elevation of 30 m; 7 flows (from TA to TG) have transitional directions and the upper 2 flows (TJ and TL), at an elevation of 150 m, have a reverse polarity. We were unable to

sample between altitudes of 150 to 250 m in this section. At 250 m (section 1, Figure 1), one flow of normal polarity (TU) was found overlying two flows (TR and TT) with intermediate directions.

The last section (R1) showed a new polarity transition. From an elevation of 50 m above sea level to 170 m (flows R1A to R1S), a reverse polarity zone was observed, overlain by a small transition zone (20 m thick) composed of 3 flows (R1T, R1U, R1V). The intermediate direction of the flow R1V is similar to that of flow TR which had been sampled at the top of the section T. Above the flow R1V, the last flow PL has a normal polarity like flow TU at the top of the section 1.

From this sampling, a synthetic cross-section of the valley has been constructed (Figure 2), which shows the stratigraphic order and the geomagnetic polarities recorded. According to the radiometric dating and the polarities observed, we have sampled the Brunhes-Matuyama reversal at the top of the volcanic sequence, followed down-section by the upper and lower Jaramillo event boundaries and the Cobb Mountain event.

LABORATORY PROCEDURES

Remanence

Each core was cut in standard specimens (2.5 cm). Remanent magnetization was measured using a Schonstedt spinner magnetometer. Stepwise demagnetizations either thermal or by alternating field (AF) were performed, at least on one sample of each core, using a Schonstedt furnace and AF demagnetizer. Most of the normal and reverse samples were cleaned only by AF demagnetization while samples from the transition zones were demagnetized with thermal or AF techniques. Flows with intermediate directions have lower NRM intensities and even though the viscous remanent magnetization (VRM) overprint is almost the same as with normal or reverse magnetized flows, the relative effect on the initial NRM is greater. AF demagnetizations were more efficient in removing isothermal (IRM) components, while thermal demagnetizations were better in cleaning viscous remanent magnetization (VRM) from weakly magnetized samples.

Primary components were easily identified and some typical demagnetization diagrams are illustrated in Figure 3.

Susceptibility

Weak field susceptibilities were measured using the Bartington susceptibility meter, at room temperature. Strong field thermomagnetic measurements were performed in vacuum (10^{-2} Torr) or in air, using an automatic recording Curie balance. Heating and cooling rates were 8°C per minute, with an applied field of between 0.1 to 0.7 Tesla.

Paleointensity

Paleointensity determinations were performed using the original Thellier's double heating method [Thellier and Thellier, 1959], which is more accurate than several other methods for basalts [Coe and Grommé, 1973]. Samples were heated in a quartz tube surrounded by a coil which produces the external laboratory magnetic field. The entire system was shielded from the geomagnetic field by 3 layers of mu-metal cylinders. Following Khodair and Coe [1975], the heatings were performed in vacuum (10^{-2} Torr) in order to minimize temperature-induced alterations of the magnetic minerals of the samples.

As with the original Thellier method, at each temperature step the two successive heatings and coolings were performed in the presence of the artificial laboratory field, but the direction of this field was reversed between each heating. This method differs a little from the modified version proposed by Coe [1967a,b] for which the first heating of each temperature step was made in zero field and the second heating in the laboratory field. The artificial laboratory field was applied during the complete temperature cycle [Levi, 1975]. The applied fields varied from 9 to 40 microteslas, in order to minimize differences between laboratory and ancient field strength [Kono and Tanaka, 1984].

PALEOMAGNETIC RESULTS

Remanence directions

When only stepwise AF cleaning was used to demagnetize a lava flow, the mean direction was calculated at the one peak of the alternating field which provided the best grouping in the data. When both thermal and AF cleanings were performed on the same flow, primary remanence directions were obtained by interpretation of Zijderveld diagrams. For these young lava flows, the primary

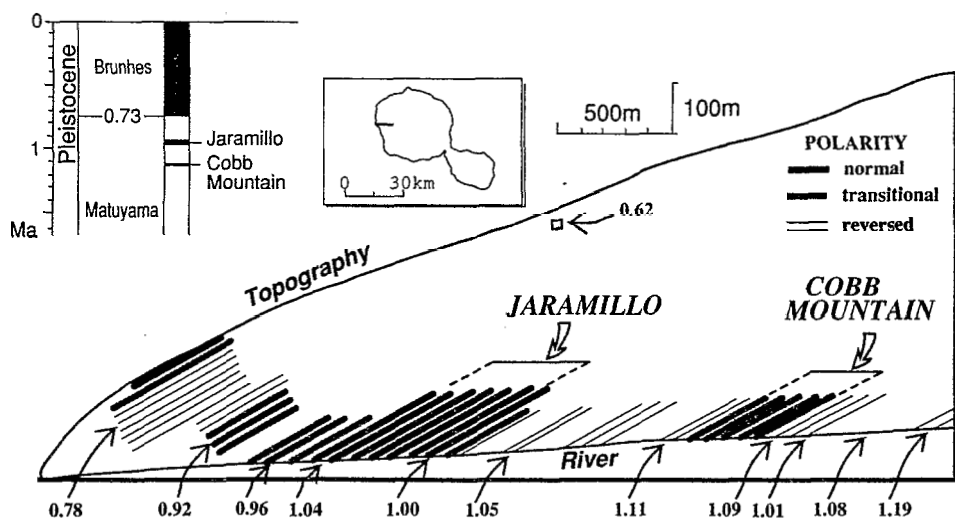


Fig. 2. Schematic cross section showing the magnetostratigraphy of the volcanic sequence, and the corresponding K-Ar age determinations.

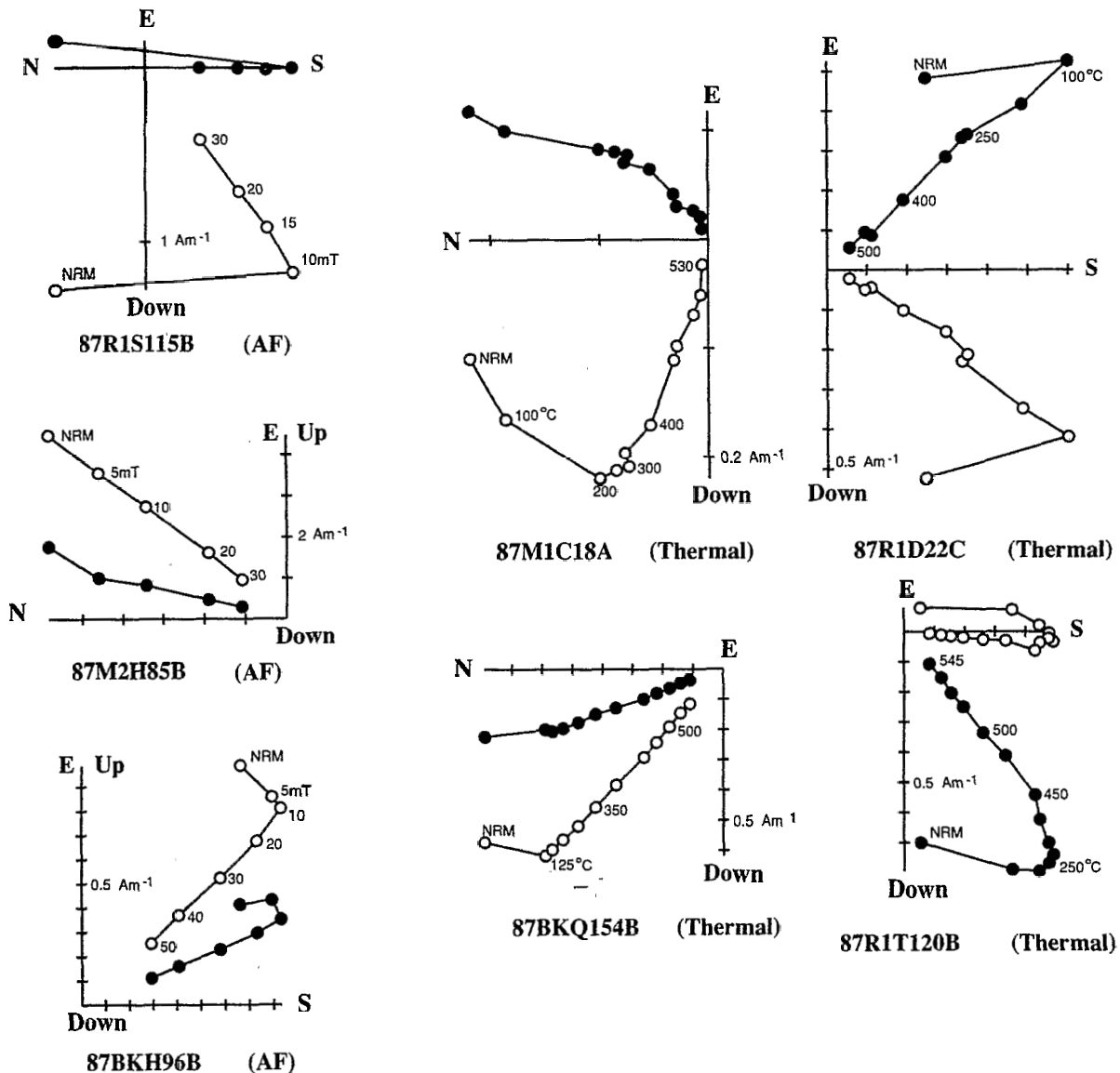


Fig. 3. Typical orthogonal diagrams of progressive thermal (TH) or alternating field (AF) demagnetizations of normal, reverse and intermediate samples. Filled circles correspond to the projection onto the horizontal plane while open symbols are projections onto the vertical plane. As seen in these plots the secondary magnetization is mainly a north component suggesting a viscous overprinting in the recent Brunhes normal polarity period. The primary component is always well defined either with thermal or AF demagnetization.

component was considered as passing through the origin. In computing mean direction per flow, we omitted anomalous cores whenever field notes indicated possible orientation mistakes, or when their directions were at more than 2 standard deviations from the mean direction of the flow. Only three flows failed to provide a reliable paleomagnetic direction. In the case of the flow M2E, neither AF nor thermal demagnetization was able to isolate a stable primary remanence. This flow belongs to the upper Jaramillo transition, and has a very weak intensity of magnetization with an overprint of higher intensity than the primary remanence. Another flow from the Jaramillo termination, TI, showed a strong overprint. Samples from this flow have an unusually high remanence intensity (more than 100 Am^{-1}) and show a very quick drop in intensity for small peak AF values (5 to 10 mT). For higher AF peaks, the intensity decrease is lower, but the directions do not change up to 100 mT, which is the maximum field of our AF demagnetizer. The scatter observed in

the directions as well as the high intensity suggest that the overprint of this flow is an isothermal remanent magnetization (IRM) due to lightning. It was obvious in the field that flow BKW was highly weathered. Demagnetization by AF was unable to completely remove the secondary component of magnetization, although the evolution of the remanent vector suggested a reverse polarity primary direction. On the other hand, during thermal demagnetizations the samples from this flow exploded in the furnace at temperatures above 300°C . Thus no paleomagnetic direction was determined for this flow.

Paleomagnetic results are listed in Table 2. In Figure 4, flow mean inclinations, declinations, and virtual geomagnetic poles (VGP) are plotted as a function of the stratigraphic position in the valley section. The altitudes reported on the right side of Figure 4 have been calculated from the thickness of the lava flows, their average dip, their true altitude and their location in the section. The stratigraphic order of the flows has been well observed in the field,

TABLE 2. Paleomagnetic Results

Site	<i>n</i> / <i>N</i>	AF/TH	<i>Dec</i>	<i>Inc</i>	<i>k</i>	α_{95}	δ	<i>Lat</i>	<i>Long</i>	<i>P</i>	<i>J</i> ₁₀	χ	<i>Q</i>
TU	5/5	200	358.6	-50.6	117	7.1	18.1	76.3	35.6	N	2.74	2.16	4.56
PL	6/6	AF+TH	2.0	-43.6	92	7.0	11.2	82.0	17.5	N	2.18	3.45	2.27
TT	6/6	AF+TH	232.9	--5.5	900	2.2	117.0	-34.0	104.6	I	0.72	2.32	1.11
TR-TS	5/6	AF+TH	230.2	0.2	1055	2.4	122.9	-37.7	106.4	I	0.75	N.d	N.d
R1V	5/6	AF+TH	235.0	0.1	42	12.0	119.0	-33.1	108.6	I	0.47	N.d	N.d
R1U	4/5	AF+TH	224.5	7.3	702	3.5	131.7	-44.2	108.1	I	1.30	N.d	N.d
R1T	5/6	AF+TH	226.6	5.4	264	4.7	128.8	-41.9	107.9	I	1.26	2.36	1.92
R1S	6/6	AF+TH	176.7	53.4	101	6.7	159.0	-73.5	220.3	R	1.88	1.37	4.93
R1R	6/6	100	185.3	44.8	231	4.4	167.1	-80.0	182.1	R	4.18	1.40	10.74
R1Q	5/6	100	182.6	50.6	347	4.1	161.8	-76.2	201.3	R	2.61	0.93	10.10
R1P	6/6	100	181.1	44.9	579	2.8	167.6	-81.2	204.2	R	6.01	1.40	15.44
R1O	6/6	200	177.1	39.7	691	2.5	172.5	-84.4	239.5	R	6.14	1.34	16.39
R1N	6/6	100	178.2	33.3	405	3.3	178.3	-88.2	284.6	R	19.47	1.69	41.40
R1M	5/5	100	176.2	36.7	724	2.8	174.8	-85.5	262.6	R	7.37	1.45	18.20
R1L	5/5	200	175.2	36.5	907	2.5	174.4	-84.8	270.0	R	11.72	1.03	40.87
R1K	9/11	200	179.8	36.6	311	2.9	175.9	-87.3	214.6	R	9.48	1.04	32.7
R1J	6/6	200	174.9	39.4	1940	1.5	172.0	-83.3	255.7	R	7.98	1.73	16.53
R1I	6/6	100	176.9	14.2	367	3.5	161.4	-79.1	14.1	R	8.32	2.78	10.76
R1H	6/6	300	179.0	11.0	327	3.7	158.4	-77.8	25.9	R	5.99	3.77	5.71
R1G	7/8	200	191.6	21.6	115	5.6	165.0	-77.0	92.1	R	6.48	1.87	12.43
R1F	6/6	AF+TH	193.2	26.7	328	3.7	167.1	-76.8	106.7	R	5.15	1.63	11.37
R1E	4/5	AF+TH	191.3	24.7	66	11.4	167.4	-78.1	98.6	R	8.94	1.68	19.12
R1D	5/7	AF+TH	143.0	15.6	214	5.5	142.5	-52.7	310.9	I	0.80	2.23	1.3
R1C	5/6	200	185.8	37.8	835	2.6	172.9	-83.5	154.1	R	2.41	1.22	7.07
R1B	5/6	200	172.2	34.8	609	3.1	173.1	-82.5	288.2	R	10.52	1.13	33.45
R1A	4/5	100	168.4	40.9	994	2.9	167.5	-77.7	270.9	R	14.17	2.89	17.61
TL	5/5	200	170.9	46.3	368	4.0	164.6	-77.0	249.1	R	4.24	1.34	11.36
TJ	6/6	200	175.3	44.6	92	7.0	167.4	-80.4	236.7	R	2.92	2.26	4.64
TI			N.d	N.d									
TG	6/6	200	133.0	74.4	249	4.2	132.3	-35.6	236.6	I	0.70	1.98	1.28
TF	7/7	200	134.0	72.5	194	4.3	133.6	-37.6	239.5	I	0.72	1.67	1.55
TE	3/5	200	297.0	42.9	299	7.1	94.9	15.3	153.7	I	0.74	2.28	1.16
TD	3/4	200	299.6	42.6	354	6.6	93.3	17.5	154.6	I	0.92	1.27	2.61
TC	8/8	200	301.3	41.5	259	3.4	91.6	19.3	154.7	I	1.04	1.87	2.01
TB	5/8	200	312.7	39.2	128	6.8	84.1	28.9	159.5	I	1.26	3.07	1.47
TA	8/8	200	337.8	35.0	83	6.1	70.9	46.7	178.1	I	1.30	2.71	1.72
M1F	6/6	AF+TH	18.2	26.0	261	4.2	61.1	53.8	241.5	I	0.20	2.41	0.30
CU	3/5	AF+TH	37.2	14.1	75	14.3	58.6	45.6	269.7	I	0.74	2.17	1.22
M1E	4/5	AF+TH	17.0	44.9	126	8.2	79.0	42.8	231.5	I	1.21	N.d	N.d
M1D	6/6	AF+TH	51.6	59.8	123	6.1	101.6	14.5	248.5	I	0.16	1.93	0.30
CT	5/5	AF+TH	66.7	50.2	19	19.3	101.5	9.6	263.6	I	0.20	1.35	0.53
CS	4/5	AF+TH	53.0	57.7	20	20.9	100.6	15.1	251.1	I	0.15	1.88	0.29
M1C	6/6	AF+TH	56.1	62.0	101	6.7	104.7	10.3	248.5	I	0.18	1.16	0.56
M1B	6/7	AF+TH	55.9	51.2	19	15.8	97.1	17.0	258.0	I	0.13	1.25	0.38
M1A	6/7	AF+TH	69.8	54.8	77	7.7	105.8	5.3	260.9	I	0.29	1.83	0.57
M2V	6/7	AF+TH	231.1	20.5	34	11.6	133.2	-40.1	119.6	I	0.38	3.43	0.39
M2W	5/5	AF+TH	238.3	12.3	92	8.0	123.2	-32.0	116.8	I	0.39	2.51	0.55
M2A	6/6	AF+TH	12.7	35.0	120	6.1	68.6	51.0	229.8	I	0.72	1.46	1.76
M2B	6/6	AF+TH	220.4	69.6	172	5.1	136.7	-42.6	178.9	I	0.39	2.99	0.46
M2C	6/6	AF+TH	213.5	58.0	194	4.8	146.0	-54.1	163.3	I	0.27	N.d	N.d
M2D	5/6	AF+TH	226.3	58.1	98	7.8	139.9	-44.7	158.1	I	0.43	N.d	N.d
M2E			N.d	N.d									
M2F	5/5	AF+TH	30.7	-4.4	401	3.8	40.2	56.1	276.8	I	0.53	N.d	N.d
M2G	6/6	AF+TH	9.0	-29.8	884	2.3	8.2	81.2	290.6	N	2.57	0.96	9.65
M2H	6/7	200	15.8	-37.3	318	3.8	13.8	74.7	315.1	N	3.58	2.81	4.57
CK	6/7	200	13.7	-34.7	408	3.3	11.6	76.9	309.0	N	3.97	1.37	10.37
M2I	4/5	100	13.6	-39.7	401	4.6	13.1	76.3	323.6	N	2.80	1.07	9.42
M2J	4/5	200	7.6	-44.0	137	7.9	12.9	79.3	350.8	N	3.92	1.82	7.73
M2K	5/6	300	4.9	-32.6	101	7.6	4.1	85.3	301.6	N	1.73	0.59	10.57
CI	5/5	200	359.8	-26.4	261	4.7	6.1	86.3	207.0	N	3.53	1.36	9.32
CH	4/5	200	358.3	-25.2	537	4.0	7.5	85.3	190.0	N	9.70	2.06	16.91
CG	4/4	200	355.0	-20.4	1005	2.9	12.9	81.4	175.7	N	3.58	0.86	14.95
M2L	6/6	100	1.6	-19.9	174	5.1	12.7	82.4	22.6	N	2.49	0.79	11.32
M2M	6/6	100	359.7	-19.7	462	3.1	12.8	82.4	208.3	N	4.17	1.85	8.07
M2N	5/6	300	354.7	-13.5	385	3.9	19.6	78.0	184.5	N	4.89	1.23	14.29
M2O	5/6	300	355.6	-9.4	1243	2.2	23.5	76.3	191.7	N	4.69	1.75	9.64
M2P	6/6	300	356.7	-15.2	379	3.4	17.6	79.5	192.3	N	3.62	0.74	17.55
M2Q	5/6	300	2.9	-32.0	334	4.2	2.5	87.2	293.8	N	3.17	0.74	15.29
CF	7/7	200	358.6	-26.9	247	3.8	5.8	86.3	189.0	N	3.11	1.61	6.92

TABLE 2. (continued)

Site	<i>n</i> / <i>N</i>	AF/TH	<i>Dec</i>	<i>Inc</i>	<i>k</i>	α_{95}	ϑ	<i>Lat</i>	<i>Long</i>	<i>P</i>	<i>J</i> ₁₀	χ	<i>Q</i>
M2R	6/6	100	0.4	-27.8	299	3.9	4.8	87.0	218.1	N	3.48	2.85	4.39
CE	6/8	200	10.7	-21.2	153	5.4	14.8	77.7	269.1	N	5.16	2.27	8.16
M2S	4/6	200	16.2	-18.6	2261	1.9	20.1	72.3	275.3	N	7.73	2.71	10.24
CD	5/5	200	19.6	-14.8	251	4.8	25.1	68.4	275.1	N	9.25	2.83	11.74
CC	4/4	200	1.9	-27.3	1395	2.5	5.0	86.6	243.0	N	3.92	1.26	11.18
CB	6/8	200	6.0	-17.8	140	5.7	15.7	79.8	246.1	N	3.93	1.65	8.55
M2T	7/7	200	7.1	-19.0	270	3.7	15.0	79.5	252.5	N	5.14	1.78	10.35
M2U	7/7	TH+AF	12.3	-19.8	1163	1.8	16.8	75.9	270.1	N	5.97	1.78	12.03
CA	5/5	200	10.6	-29.7	520	3.4	9.5	79.7	292.3	N	7.11	1.03	24.79
PN	7/7	200	354.6	-36.5	102	6.0	6.0	84.3	92.7	N	7.00	2.68	9.37
PM	6/7	100	10.4	-33.3	232	4.4	8.8	80.1	305.0	N	5.14	2.59	7.13
PJ	5/5	200	0.8	-40.4	413	3.8	7.9	84.6	22.8	N	4.47	3.64	4.40
PI	6/6	200	359.3	-34.0	210	4.6	1.6	88.8	65.9	N	3.16	3.21	3.53
PH	7/7	200	1.9	-17.3	278	3.6	15.3	81.0	222.6	N	4.37	1.66	9.45
PG	7/7	200	6.4	-31.6	258	3.8	5.5	83.9	296.0	N	3.84	1.18	11.66
PF	8/8	AF+TH	157.8	55.8	233	3.6	152.8	-62.9	252.6	I	1.29	1.95	2.38
PE	8/8	AF+TH	158.6	57.1	102	5.5	151.3	-62.6	249.4	I	2.40	0.90	9.55
PC	7/7	100	179.4	74.4	297	3.5	138.1	-46.9	211.0	I	1.39	0.39	12.83
PB	7/7	200	182.6	63.9	175	4.6	148.6	-62.0	206.7	I	2.63	0.38	24.75
PO	6/6	100	174.4	47.8	158	5.4	164.2	-77.7	234.3	R	3.36	0.98	12.31
PA	7/7	300	187.4	36.8	85	8.8	172.6	-82.5	143.7	R	3.33	0.71	16.78
PKG	4/5	AF+TH	183.8	27.5	407	4.6	174.0	-85.2	80.7	R	14.87	1.01	52.71
PKE	5/5	AF+TH	179.3	27.5	273	4.6	174.9	-86.8	18.3	R	20.37	1.25	58.41
BKZA	9/9	AF+TH	178.7	28.2	132	4.5	175.5	-87.0	5.6	R	3.32	1.93	6.19
BKZ	4/8	AF+TH	196.2	32.6	106	9.0	166.4	-74.6	123.2	R	3.27	1.09	10.83
BKY	6/7	AF+TH	185.2	25.0	757	2.4	171.2	-83.2	78.9	R	1.13	2.35	1.73
BKX	11/12	AF+TH	175.4	41.5	504	2.0	170.3	-82.5	244.7	R	2.25	1.80	4.48
BKW			N.d	N.d									
PKB	5/7	AF+TH	155.5	48.4	67	9.4	155.7	-64.8	268.5	R	0.53	2.82	0.68
BKS	7/7	AF+TH	156.5	47.6	492	2.7	156.7	-65.8	269.3	R	1.14	1.93	2.11
BKT2	6/6	AF+TH	332.4	27.7	70	8.0	65.7	47.7	168.9	I	0.72	1.51	1.71
BKT1	5/5	AF+TH	358.7	45.8	87	8.2	78.4	45.1	209.0	I	0.95	2.44	1.40
BKR	5/6	AF+TH	342.1	44.5	212	5.3	78.7	42.8	188.5	I	0.85	N.d	N.d
BKQ	6/6	AF+TH	339.6	60.5	31	12.3	94.5	27.9	193.4	I	0.50	1.19	1.51
PKD	5/6	AF+TH	339.9	45.8	213	5.3	80.4	41.0	186.7	I	0.56	0.97	2.07
BKP	7/7	AF+TH	348.1	28.7	992	1.9	62.3	55.0	190.3	I	0.53	0.87	2.18
BKO	7/7	AF+TH	351.4	25.5	596	2.5	58.6	57.7	194.8	I	0.51	1.63	1.12
BKN	7/7	AF+TH	351.2	22.6	185	4.5	65.8	59.3	193.5	I	0.29	1.48	0.70
BKL	5/7	AF+TH	219.7	7.3	41	12.0	135.4	-48.7	105.4	I	0.62	1.88	1.19
BKK	5/5	AF+TH	221.3	-5.7	313	4.3	125.2	-44.4	97.9	I	0.92	N.d	N.d
PKC	6/6	AF+TH	220.8	6.4	272	4.1	134.0	-47.5	105.5	I	1.38	1.96	2.53
BKJ	7/7	AF+TH	220.8	5.2	242	3.9	133.2	-47.2	104.6	I	0.39	2.11	0.66
BKI	6/6	AF+TH	160.0	-40.3	924	2.2	104.9	-44.9	4.2	I	1.10	1.98	1.99
BKH	8/8	AF+TH	164.3	-48.1	42	8.6	98.1	-40.8	12.4	I	0.44	3.00	0.52
BKG	9/9	AF+TH	169.8	40.2	349	2.8	168.8	-79.1	270.3	R	1.77	0.42	1.51
BKF	7/7	AF+TH	177.2	10.6	590	2.5	157.9	-77.3	17.8	R	1.51	1.06	5.14
BKE	7/7	AF+TH	180.3	13.0	280	3.6	160.5	-78.9	32.1	R	1.60	0.22	26.02
PKA	7/7	400	184.3	17.9	378	3.1	164.9	-80.5	57.3	R	1.71	0.56	10.90
BKD	6/6	AF+TH	180.0	15.2	318	3.8	162.7	-80.0	30.6	R	2.47	0.27	32.85
BKC	6/6	AF+TH	175.9	15.1	105	6.6	162.2	-79.2	8.3	R	2.72	0.47	20.71
BKB	7/7	AF+TH	181.7	10.6	332	3.3	158.0	-77.5	38.5	R	3.52	1.02	12.43
BKA	4/5	200	186.0	16.6	678	3.5	163.2	-79.1	63.7	R	2.07	0.40	18.67
BKV	7/8	200	174.5	30.6	234	4.0	174.9	-84.6	312.9	R	2.10	3.43	2.20
DIKE													
PD	4/7	AF+TH	0.2	-36.5	69	11.1	N.d	87.4	26.5	N	N.d	N.d	N.d
BKM	6/6	AF+TH	191.7	42.2	212	4.6	N.d	-77.2	154.1	R	1.36	1.77	2.75
BKU	6/6	AF+TH	171.9	32.8	239	4.3	N.d	-82.3	298.2	R	0.62	0.25	8.81
PKF	5/5	AF+TH	24.0	-30.8	132	6.7	N.d	67.1	301.5	N	1.35	1.49	3.27

n/*N*, number of samples used in the analysis/total number of samples collected; AF/TH, AF+TH indicates that thermal and AF demagnetizations have been done, while a number refers to the AF peak (Oe), at which the mean was calculated; *Dec* and *Inc*, mean declination and inclination; *k*, precision parameter of Fisher; α_{95} , 95% confidence cone about mean direction; ϑ , reversal angle; *Lat* and *Long*, latitude and longitude of VGP; *P*, polarity of the flow (N: normal, R: reverse, I: intermediate); *J*₁₀, geometric mean NRM intensity after 10 mT; χ , geometric mean susceptibility (10^{-2} SI units); *Q* geometric mean ratio of *J*₁₀/(35 μ T $\cdot\chi$).

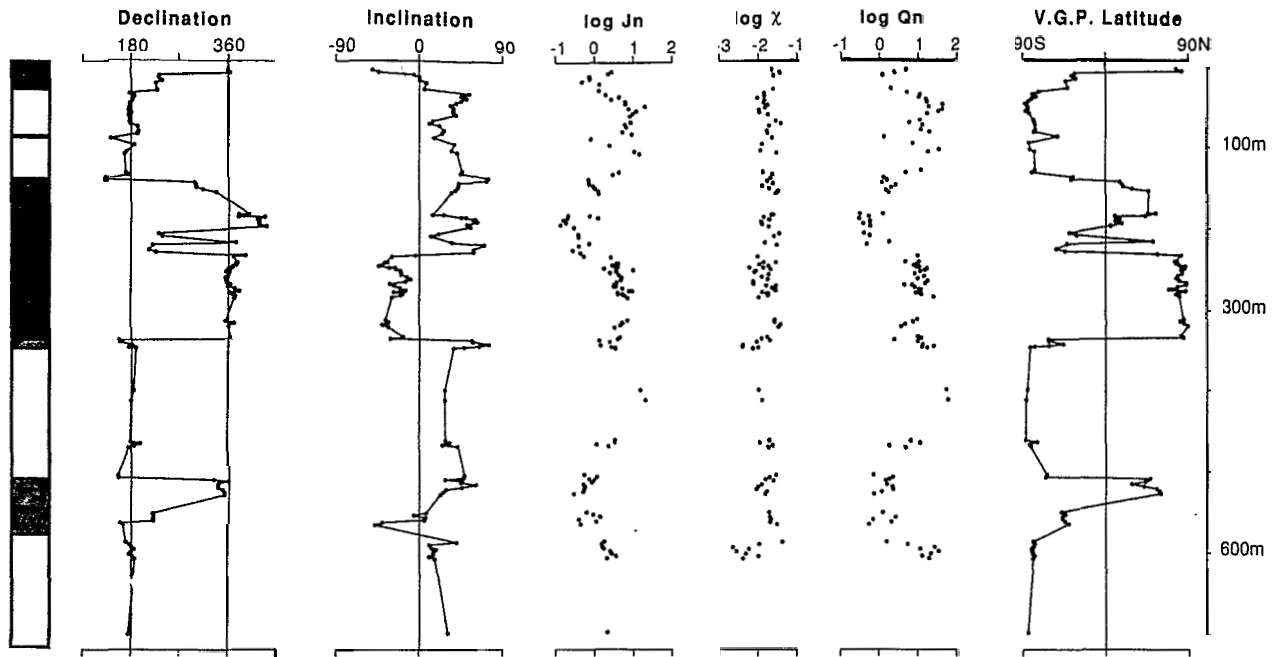


Fig. 4. Evolution of different magnetic parameters for each flow of the sequence against the calculated cumulative thickness. J_n , average NRM intensity after 10 mT; χ , mean susceptibility; Q_n , apparent Koenigsberger ratio (see text). The axial normal dipole inclination at that site is -32.5° (32.5° for reverse). While the susceptibility appears to be equivalent throughout the section, large variations in intensity are seen and the low values are always correlated to transition zones, identified on the VGP latitude plot. These low values are also well defined with the apparent Koenigsberger ratio.

both along the river and within each vertical section. To match the relative positions of the flows between different vertical sections, field observations of flow attitudes were often sufficient. For example, taking into account the distance between section M1 and M2 (see Figure 1) and the dip of the flows toward the west, the top-most flow of section M2 (flow M2V) is stratigraphically beneath the bottom flow of section M1 (flow M1A). The same arguments were applied to sections T and R1 (Figure 1) and the flow TL (section T) is lower in the stratigraphy than flow R1A (beginning of section R1). This stratigraphic assignment is in good agreement with the resulting sequence of magnetic polarities. In two cases, only paleomagnetic correlations have been used. First, section 2 (CS, CT, CU) and section M1, which are close to one another in the field, have similar paleomagnetic directions which suggests that flows CS, CT, CU are in the same stratigraphic level as flows M1A to M1D (CS: $D=53.0$, $I=57.7$; CT: $D=66.7$, $I=50.2$; M1D: $D=56.6$, $I=59.8$).

Correlations based on paleomagnetic directions are easier in the case of intermediate directions of the geomagnetic field, because they are more unique. On the contrary, it is more difficult to recognize and correlate directions during stable periods (reverse or normal) of the field. Our sections CA to CK and M2U to M2G both correspond to the Jaramillo normal subchron. Using the altitudes of the flows, their natural dip and the paleomagnetic directions, we combined the two sections. However, we cannot dismiss the possibility that the same flow was sampled at both sites. The stratigraphic order chosen on the basis of the paleomagnetic data is indicated in Table 2.

Defining the boundaries of transitions in terms of directions is not so easy. Considering a direction to be transitional only when its corresponding VGP falls below a latitude of 50° [Sigurgeirsson, 1957], or 40° [Wilson et al., 1972] is not always possible, as can be seen for example with flows BKP, BKO and BKN (Figure 4).

These flows have purely transitional directions (Table 1) which correspond to an angular departure from the axial dipole higher than 50° . Their NRM intensities are also very weak, but their corresponding VGPs have a latitude higher than 50° . It seems that a better requirement for a direction to be considered intermediate is that the reversal angle (measure of the angular departure from the normal or reverse axial dipole) would be higher than 30° . This requirement was already proposed by Hoffman [1984] and we will see later that, from our data, this cutoff between intermediate and dipolar directions is not totally arbitrary.

Figure 4 shows that the thickness of the transitional zones is greatly variable. The upper Jaramillo transition has a thickness around 80 m while the normal subchron Jaramillo has been recorded only by a sequence of 120 m. Taking into account that a transition period may be 5000 years and, that the Jaramillo subchron is 60,000 years long, great differences in the extrusion rate of the lava flows are then evident.

NRM intensity and susceptibility

The stepwise AF demagnetizations show that generally the secondary component of magnetization is cleaned at a peak AF of 10 mT. In order to define the distribution of the intensities of the primary directions, we report here the NRM intensities after 10 mT of AF cleaning (J_{10}). The NRM intensities are distributed between less than 0.1 Am^{-1} up to 30 Am^{-1} , and samples with intermediate directions clearly have lower intensities of magnetization than normal and reverse samples. In contrast, there is no apparent difference in weak field susceptibility for both populations (Figure 5); lowest values correspond to high-temperature oxidized samples. As a result, the distribution of the apparent Koenigsberger ratio, (NRM intensity after AF cleaning at 10 mT divided by the product of the bulk susceptibility by an

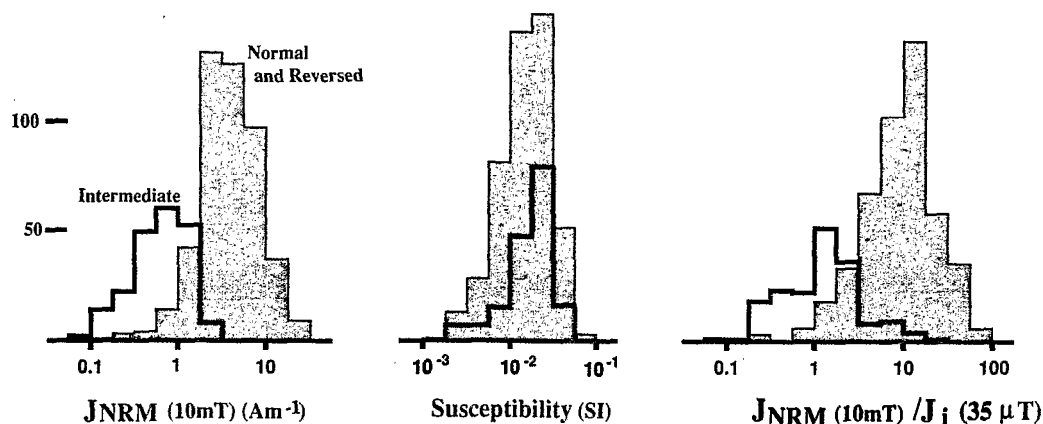


Fig. 5. Histograms showing the distribution of the NRM intensity (after 10 mT), the susceptibility, and the ratio of the previous NRM with a calculated induced magnetization in a field of 35 μT . Samples have been separated into two populations, intermediate and normal+reverse.

ambient field of 35 μT), is similar to that of the intensities of magnetization.

Geometric mean values of NRM intensities (J_{10}), weak field susceptibilities and apparent Koenigsberger ratio calculated per flow are reported in Table 2 and are represented in Figure 4. This figure clearly shows that the average NRM intensity per flow is lower during transitional periods than during normal or reverse periods. This fact is particularly clear when the transitional zone is well detailed. This pronounced decrease is also observed in the Koenigsberger ratio, because there are no differences in susceptibility between samples from the transitions and samples with a normal or reversed direction. These results strongly suggest that the variations observed in intensity of magnetization are not mineralogically controlled but reflect changes in the geomagnetic field intensity. This is easily seen when the geometric average NRM intensities, after 10 mT, are displayed versus the reversal angle in Figure 6. Although there is considerable scatter of the data, with a deviation of one order of magnitude between some flows, the distinction between flows with intermediate directions and those with stable polarity is very clear. In a study of a N-T-N

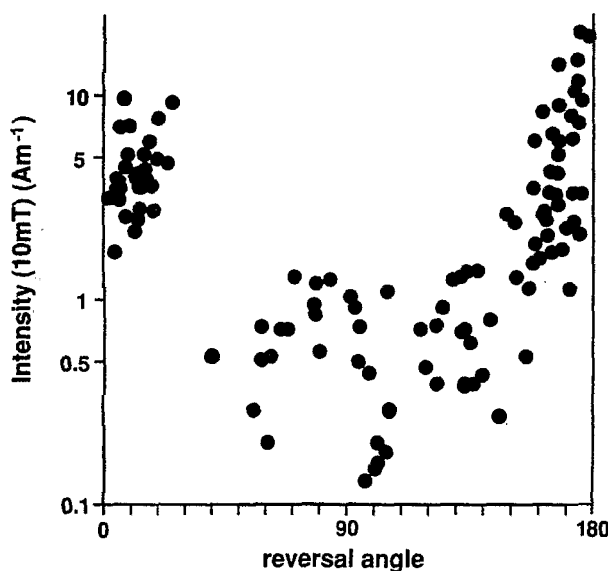


Fig. 6. Variation of the mean flow intensity of magnetization (after 10 mT) versus reversal angle. Intensity of magnetization is on a logarithmic scale.

excursion recorded on lava flows from the island of Huahine (Society islands), a similar distribution of the intensities of magnetization is observed [Roperch and Duncan, this issue]. The intensity of the geomagnetic field, during transitions, is thus expected to decrease down to 10-20% of the value observed during stable polarity states.

Nevertheless, we must emphasize that NRM intensity is a parameter which provides only a general trend of field variations, when a large number of samples and flows are used. Details in the paleointensity changes between flows can not be resolved with NRM intensities alone. Absolute values of the geomagnetic intensity are necessary in order to better constrain paleofield variation during reversals. Unlike the sedimentary and intrusive rocks, lava flows record a quasi-instantaneous field, and they can provide accurate absolute paleointensities. In order to quantify the relative change in the geomagnetic field intensity reflected by the NRM data, some paleointensity determinations were attempted and will be presented below.

STATISTICAL ANALYSIS OF THE DISTRIBUTION OF THE NORMAL AND REVERSE DIRECTIONS.

A previous study of paleosecular variation recorded in volcanic rocks from French Polynesia [Duncan, 1975] indicated the magnitude of dispersion of the paleomagnetic data was in agreement with values predicted by secular variation models, with an angular standard deviation of the site VGP's about the geographical axis of 13.8°. This result was obtained for 53 sites geographically distributed in 5 of the younger islands of the volcanic chain and representing a 4 m.y. time interval. In contrast, our sites represent a single volcanic sequence from the Punaruu valley. A statistical analysis of the dispersion of the paleomagnetic directions may provide some insight to the sampling process of the magnetic field by such a volcanic sequence.

The normal polarity data set comprises 31 flows erupted during the Jaramillo subchron, 2 during the Brunhes period and 2 dikes (Table 2). As most of the data correspond to the Jaramillo period they might represent a maximum time interval of about 60,000 years (Figure 7). The set of reversed directions is composed of 39 lava flows and 2 dikes (Figure 7) and might represent a longer interval of time (approximately 350,000 years).

First, paleomagnetic directions more than 30° away from the axial geocentric dipole were excluded from the analysis, since they have been considered as transitional. In some studies [McFadden and McElhinny, 1984; McElhinny and Merrill, 1975] only VGP

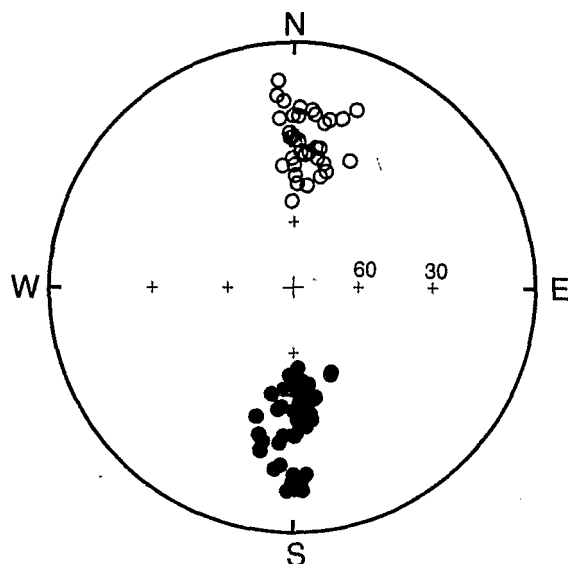


Fig. 7. Stereographic projections of all normal and reversed polarity directions observed in the volcanic sequence from Tahiti.

latitudes lower than 45° were excluded. The non-Fisherian pattern of the directions (Figures 7a,b) is common for sites at low latitudes, because of the movement of the dipole (wobble). As a consequence, the distribution of the VGPs associated with the paleomagnetic directions is much more Fisherian (Figures 8 a and b).

The mean VGP for the Jaramillo flows is: long=263.9°, Lat=84.4°, with K=87.1, ST=8.7° and $\alpha_{95}=2.8^\circ$. As was discussed during the description of the sampling, two sections composed the Jaramillo; some sites between CA to CK perhaps correspond to flows already sampled in section M2. Nevertheless, even if the ten flows between CA to CK are taken out of the computation, the result is not changed significantly (mean VGP: l=266.8° L=85.0°, K= 83.1, $\alpha_{95}=3.5^\circ$, ST=8.9°). At the 95% confidence level, the mean VGP is distinguishable from the geographical axis, and the relatively low value of the angular standard deviation of the VGPs

suggests either a low level of the non-dipole field activity, or an insufficient sampling of the secular variation possibly due to a high rate of extrusion of the lavas flows. For the Jaramillo data set, whether the flows were erupted regularly over 60,000 years or in one or a few short periods is an unanswered question.

For the reversed directions, the mean VGP is indistinguishable from the geographical axis at the 95% confidence level, but the angular standard deviation remains lower than the expected value at this latitude (mean VGP: l=268.0°, L=-88.9°, K=52.2, $\alpha_{95}=3.2^\circ$, ST=11.2°). Such statistics with a moderate number of samples, are very sensitive to the selection of the data. Adding 5 flows, with VGP latitude between 45-50°, but a reversal angle higher than 30°, the dispersion of the data is in better agreement with other models (which used this cut-off level) for the secular variation. (l=246.0°, L=-86.4°, K=30.0, $\alpha_{95}=3.9^\circ$, ST=14.8°).

The mean VGP for all the normal and reversed directions with VGP latitudes higher than 45° has an angular standard deviation very close to the expected value: l=327.9°, L=88.9°, $\alpha_{95}=2.7^\circ$, K=34.2, ST=14.0°. The angular standard deviation of the field is usually calculated with the following formula: $SF^2 = ST^2 - SW^2/n$, where ST is the total standard dispersion between sites, SW the within site dispersion and n the average number of samples per flow. The more inclusive VGP population gives a field dispersion SF=13.9° (SW=4.6°, n=5.9).

This study of the paleosecular variation provides the following conclusions:

The mean VGP associated with all the normal and reversed directions is indistinguishable from the geographical axis.

The results from the Jaramillo subchron indicate either that the Jaramillo represents too short a period of time to average the secular variation at this site or that the individual observations (i.e., each lava flow) are not independent in time and represent only a short time in the Jaramillo.

Finally, our estimate of the angular standard deviation of the VGP is identical to the value obtained by Duncan [1975] and is very close to the value given by the different models. (The most recent (G) of McFadden et al. [1988] gives SF=13.4° for the latitude of Tahiti.)

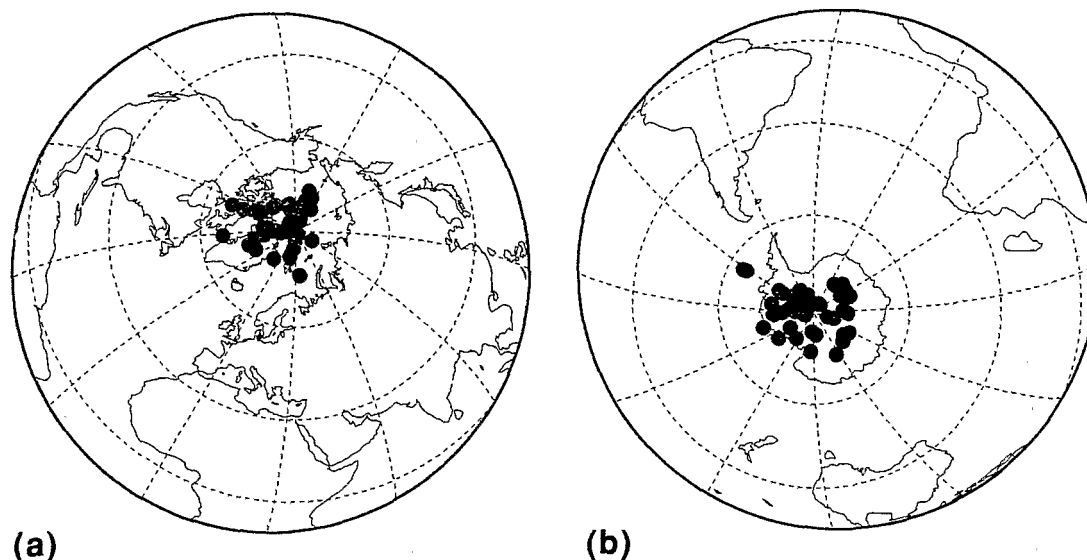


Fig. 8. Equal area projection of the VGPs corresponding to the previous directions shown on Figure 7.

DESCRIPTION OF THE TRANSITIONS

The directional path, before (D,I) and after rotation (D',I') following *Hoffman* [1984], for all the transitions found in our sequence, are displayed on stereoplots (Figure 9) while the virtual geomagnetic pole paths are shown in Figure 10.

Cobb Mountain (Figures 9 and 10)

The paleosecular variation is not well recorded in the bottom of the section because several reverse flows (BKA to BKF) have recorded statistically indistinguishable directions with low inclinations. Only the two flows (BKV and BKG) erupted before

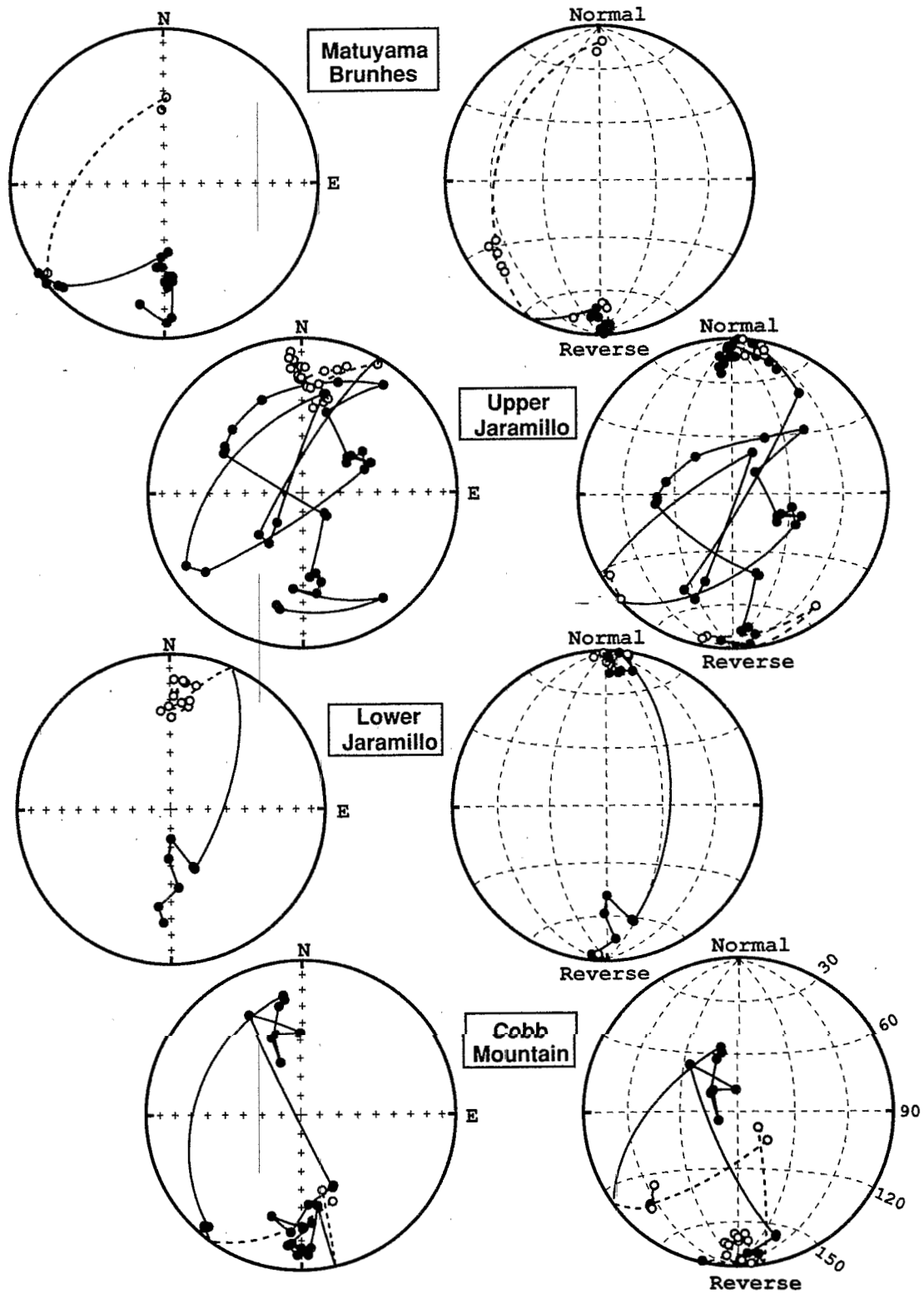


Fig. 9. For each transition, equal area projections of the directional paths before rotation (left) and rotated directions (D', I') [*Hoffman*, 1984] (right).

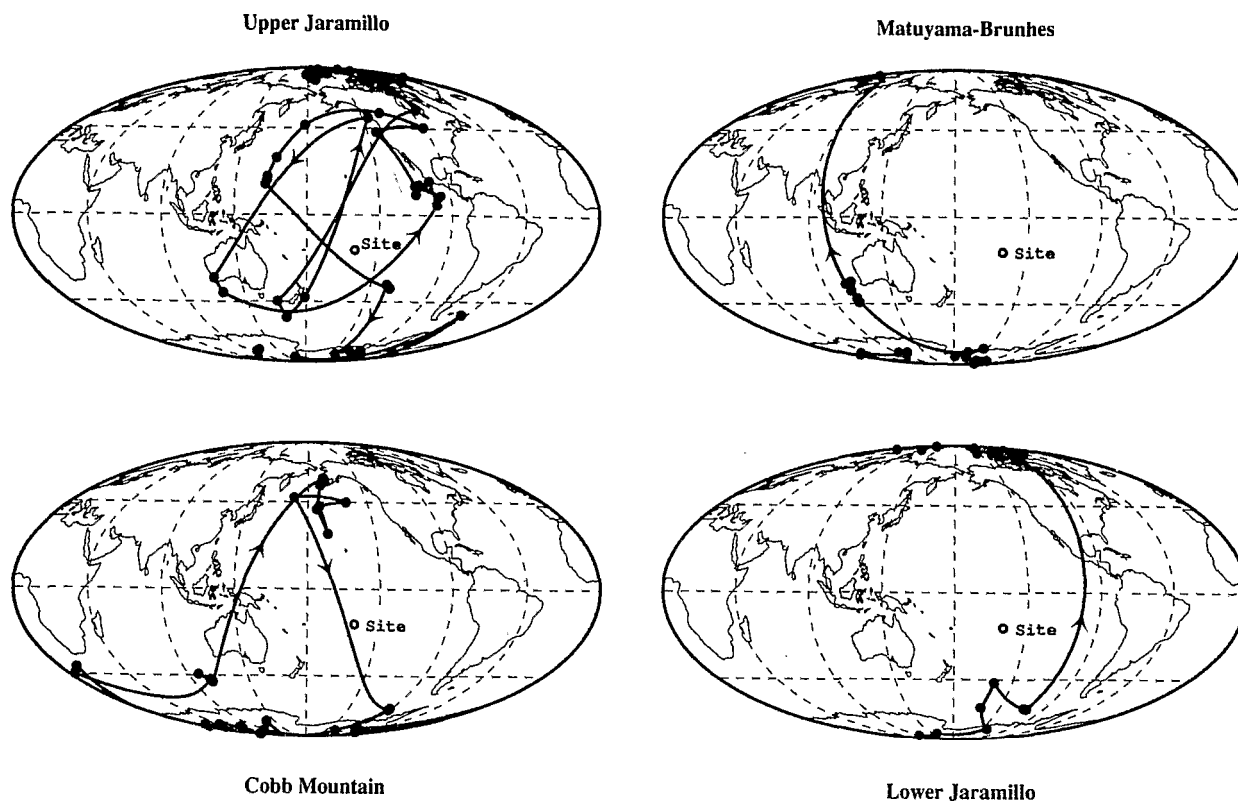


Fig. 10. Evolution of the VGPs during each transition plotted on a Mollweide projection. Same data sets as in Figure 9.

and after this group have different directions. As discussed before, there is a few tens of meters gap in the sampling between the last reversed flow (BKG) and the next (BKH) which is intermediate. Thus, the flow BKH might not correspond to the precise beginning of the transition but may record a direction well advanced in the transition and the apparent far-sided VGP movement to position about 160° away from the site meridian should be interpreted cautiously. After that, southwest directions (flows BKJ to BKL) associated with shallowed inclinations have been recorded by 4 successive flows. The VGPs associated with these directions cannot be easily classified as near or far-sided. The following directions (flows BKN to BKT2) are north but with positive inclinations between 20 and 60° ; in the D' , I' space they are situated in the near-sided quadrant, and are 90 to 60° away from the reverse polarity direction while the VGPs are closer to normal polarity. Just above these intermediate directions, a direction only 25° away from the reversed polarity was recorded by two successive flows. Even though there are some gaps in the sampling, the overlying flows also have reversed polarity. No normal directions were observed, so this record is an apparent R-T-R excursion. K-Ar dating of five flows from this part of the sequence (Table 1) yields a weighted mean age of 1.11 ± 0.01 Ma and indicates that this excursion should be correlated to the Cobb Mountain event [Mankinen et al., 1978].

Lower Jaramillo (Figures 9 and 10)

The transition is not well sampled; 4 flows (Table 2) have a paleomagnetic direction which involves a steepening in the inclination and are followed above by normal polarity flows. In contrast with what is observed for the other transitions, the NRM intensity of these 4 flows cannot be distinguished from that of the underlying flows. This fact suggests that these flows recorded the

beginning of the transition. No accurate paleointensities are available to confirm this interpretation.

Upper Jaramillo (Figures 9 and 10)

This reversal boundary is much more detailed and is recorded by 23 flows. The first transitional direction (flow M2F) has a very shallow negative inclination, and shows a large swing of the field away from its secular variation pattern during the Jaramillo subchron. A different direction (southwest and steep positive inclination) is observed in the three following flows (M2D, M2C, M2B). The next transitional direction (M2A) is north with a moderate positive inclination, and it is followed by two southwest directions (flow M2V, M2W). There is no gap in the sampling of these flows. Another transitional direction (east and positive steep inclination) has been recorded at six sites (M1A, M1B, M1C, CS, CT, M1D). The possibility that a gap in the sampling exists between section M2 and section M1 cannot be ruled out. Then, a movement of the directions to the north with a decrease in inclination is observed (M1E, CU, M1F). In contrast with this irregular behavior, flows TA to TE exhibit a smooth shift in direction which seems to correspond to a better sampling in time of the field variation or a more regular behavior of the field. The end of the transition shows steep and southeast directions (flows TF and TG). The VGPs associated with these intermediate directions are grossly near-sided except for two (flows M2V and M2W). All the transitional directions are associated with a weak NRM intensity.

The next 5 flows (TJ, TL, R1A to R1C) are reverse directions, with NRM intensities higher, and characteristic of the stable polarity state. But, the next flow above (R1D) has a remanent direction which goes out of the typical secular variation pattern, with an angular departure from the axial dipole of 37° and low

intensity of magnetization. This special direction was obtained during thermal demagnetization as well as with AF cleaning, and is well determined as shown by sample 87R1D22c on Figure 3. This site was clearly identified as a lava flow and not a sill.

Our record of the Upper Jaramillo is clearly characterized by: *i*) large changes between two intermediate directions (i.e., between the flows M2A and M2W), *ii*) progressive vector movement of the field, recorded by successive lava flows (flows CU to TE), and *iii*) relative stability in intermediate positions (flows M1A to CT). The question is: are these properties related to the transitional field behavior or are they just an effect of the sporadic extrusion of the lava flows? Quick and large directional changes can be attributed first to gaps in the paleomagnetic sampling. We have seen that this is not the case however, for the three larger vector movements recorded by the flows of the top of section M2. Gaps due to changes in the extrusion rate are more difficult to verify.

There is evidence that the intensity of the Earth's magnetic field during the transition was very low, as shown by the NRM intensity and also the paleointensity data (see next section). With a small magnetic vector, large and sudden changes in direction are easier to produce than with a normal geomagnetic field intensity. A simple model of reversals, in which the dipole term of the spherical harmonic expansion is reduced to zero while the other terms are allowed variations in 'realistic' agreement with the present non dipole field, gives a record also characterized by periods of progressive changes and periods of important and rapid directional variations when the magnetic field intensity is greatly reduced [Roperch, 1987]. Similar behavior is also observed in the recent reversal models proposed by Williams *et al.* [1988]. Therefore the observed features of our record of the Upper Jaramillo transition might not be entirely controlled by the sporadic volcanic activity, and some of them might reflect the irregular evolution with time of the local field directions during intermediate states. Nevertheless, it is obvious that we do not have a complete record of changes in the paleomagnetic directions during the transition, as expected with volcanic rocks [Weeks *et al.*, 1988].

Matuyama-Brunhes (Figures 9 and 10)

Before the Matuyama-Brunhes boundary, a progressive increase in inclination is observed and we speculate that this pattern has some similarities with the Lower Jaramillo. The transition is not detailed and only five lava flows have recorded intermediate directions which are southwest with a shallow inclination and 50° to 60° away from the geocentric axial dipole.

PALEOINTENSITY DETERMINATIONS

The aim of the Thellier method is to compare partial thermoremanent magnetization (PTRM) acquisition and the decrease of the partial natural remanent magnetization (PNRM) with increasing temperature steps. Because of the law of additivity of the PTRM, the ratio PNM/PTRM should be constant over each temperature interval and equal to the ratio of the ancient field strength and the laboratory field, provided no alteration of the magnetic minerals occurred during the heating. Only samples whose NRM is an original TRM, with no significant secondary magnetization, and showing no or little thermal instability, enable a paleointensity determination.

Sample selection

To select the most suitable samples for the paleointensity measurements, we used the following criteria: the NRM direction, the magnetic mineralogy and the thermal stability of the magnetic minerals.

NRM direction. The NRM direction must be close to the mean stable direction for the flow obtained after AF and/or thermal demagnetization. This allowed us to reject samples carrying significant viscous remanences (VRM). This criterion was particularly efficient for samples with a transitional direction, whose primary remanent magnetization was very weak, and the overprint was often relatively more important than for samples with a non-transitional direction.

Grain size. Multidomain grains cause non-ideal behavior during the Thellier experiment, and a concave up curvature of the points in the NRM-TRM diagram [Levi, 1977]. This effect prevents the use of the low-temperature part of the NRM-TRM diagram to calculate the paleointensity, because the slope of the line would be steeper than those provided by the ratio of the true paleointensity to the laboratory field.

Remanence stability to AF demagnetization with median demagnetizing fields above 30 mT. was used to indicate that the remanence is controlled by single (SD) or pseudo-single (PSD) domain particles. These experiments were performed on adjacent specimens from the same core.

Thermal stability. Thermal stability of our samples was investigated with strong field thermomagnetic experiments. The degree of alteration during the Js-T experiments was estimated from the difference between the Curie point on heating and that on cooling and also from the change in the strong field induced magnetization (Js) at room temperature before and after heating. It is well known that volcanic rocks with a single high Curie temperature are good candidates for paleointensity determinations because their highly oxidized state generally prevents a further oxidation during the laboratory experiment. Js-T experiments, performed on 111 samples, exhibit four types of curves (Figure 11). We assumed that the Curie temperature corresponds to the temperature of the inflection point of the Js-T curve. This method yields values generally lower than those obtained using a linear extrapolation of the Js-T curve as described by Grommé *et al.* [1969]. The temperature of the inflection point can be considered as the average of the broad distribution of the Curie point of the individual magnetic particles within a volcanic rock [Prévoit *et al.*, 1983].

The first type of Js-T curves is the most common encountered (76 samples) and shows a single ferrimagnetic phase, with a high temperature Curie point between 500 and 565° C. The type 1 curve can be divided into three groups, according to the relative discrepancy between the heating and cooling curves. Samples of group 1a are characterized by a decay of the strong field induced magnetization at room temperature, Js, after the heating, less than 10% and a decrease of the Curie temperature during the cooling of only a few degrees. This behavior has been found on 42 samples. Group 1b (13 samples) shows a decrease in Js greater than 10% after the heating and a more important drop of the Curie temperature during the cooling. The evolution of the samples is more pronounced when heatings are made in air than in a vacuum. The group 1c (21 samples) is characterized by an increase in the induced magnetization at room temperature after heating, since the cooling curves cross the heating curves, typically in the temperature interval 250-450°C. The magnetic phase producing the type 1 curve could be a titanium-rich titanomagnetite which has been transformed to a Ti-poor titanomagnetite by high temperature deuteric oxidation, or a primary low-Ti titanomagnetite. Discrepancies between the groups 1a, 1b and 1c might result either from low temperature oxidation which induces non-reversible behavior or minor variations in the magnetic grains or bulk rock [Mankinen *et al.*, 1985].

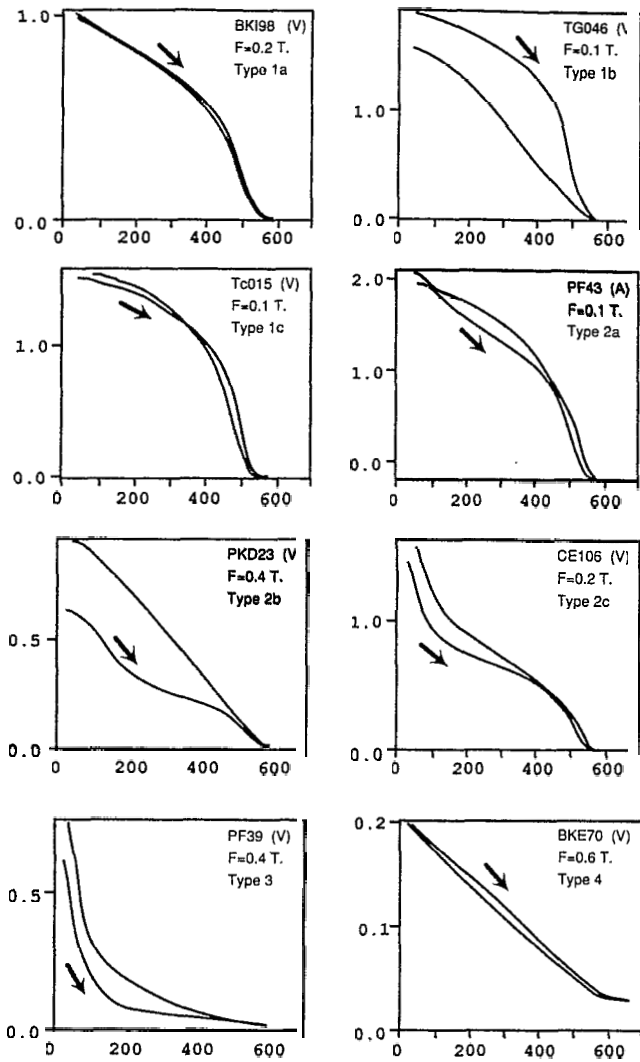


Fig. 11. Examples of the four different types of strong field thermomagnetic curves obtained on samples from the island of Tahiti. Analyses were done either in a vacuum (V) or in air (A) with various applied fields from 0.1 to 0.6 Teslas. Arrows indicate heating curves. The unit of the specific magnetization is given in $\text{Am}^2\text{Kg}^{-1}$.

Type 2 curves were produced by 14 samples and they result from the presence of two ferrimagnetic minerals. These curves can also be separated into 3 classes. In class 2a (8 samples), one magnetic phase commonly has a Curie point between 100 and 200°C, while the other phase has a Curie temperature higher than 500°C, but the heating and cooling curves are nearly reversible. In contrast to the previous class, class 2b (9 samples) shows irreversibility, the cooling curves always being above the heating curves. Class 2c curves (7 samples) are also characterized by two Curie points; one above 500°C and the second lower than 100°C and in some cases lower than the room temperature. In all cases, the Curie points of samples were changed only by a few degrees after the experiment. Bimodal Curie temperature samples are commonly observed in flows where high temperature deuteric oxidation has transformed only part of an originally Ti-rich titanomagnetite to a Ti-poor titanomagnetite containing ilmenite lamellae. The non-reproducibility of the heating and cooling curves of group 2b indicates a low temperature oxidation and the lower Curie point might be a cation deficient titanomaghemite but the disproportionation peak has been observed in only one sample.

Type 3 curves show only one ferrimagnetic mineral with a very low Curie temperature, below 75°C and sometimes lower than the room temperature. The cooling curves do not retrace the heating curves with heating performed either in air or in vacuum. Seven samples produced this kind of curves.

Only 3 samples gave type 4 Js-T curves. This type of curve shows some paramagnetic behavior due to the highest applied field and these samples have low magnetic content as indicated by the low value of the magnetic force.

As the Js-T experiments were carried out on selected samples without large secondary magnetization, they do not represent the true distribution of the Curie points over the entire flow sequence. For the paleointensity measurements, we have used only samples exhibiting type 1 Js-T curves.

Interpretation of the NRM-TRM diagrams

The paleointensity data are shown in NRM-TRM diagrams [Nagata *et al.*, 1963] where the NRM (y_i) remaining at each temperature step (t_i) is plotted against the TRM (x_i) acquired from t_i to room temperature in the laboratory field. Ideally all points should be on a straight line whose slope gives the ratio between the intensity of the ancient geomagnetic field and the laboratory field, but generally, only one part of the diagram is linear. The temperature at which the secondary magnetization, such as VRM, is cleaned, determines the lowest limit of the temperature interval which can be used for paleointensity determinations. Because a linear distribution of the points on the NRM-TRM diagram is not a proof of the absence of chemical or physical changes during the Thellier experiment [Prérot *et al.*, 1983], we have to check the stability of the partial TRM acquisition capacity as the heating temperature increases (PTRM checks). Any increase or decay in the TRM acquisition capacity indicates a physico-chemical alteration of the magnetic minerals.

Generally, several PTRM checks were performed during each experiment using larger temperature intervals with increasing heating temperature. The acquisition of chemical remanent magnetization (CRM) during the heating in the laboratory field cannot always be detected by the PTRM checks [Coe *et al.*, 1978], but when the laboratory field and the NRM are not parallel, a movement of the NRM direction toward that of the applied field shows an alteration in the TRM spectrum due to CRM build up. This is easily checked on the orthogonal plots of the NRM demagnetization in sample coordinates. At each temperature step, the first heating is the most efficient in producing chemical changes. This has been verified in measuring the bulk susceptibility at room temperature after both heatings at each step. Small changes in susceptibility are observed after the first heating of each temperature step, while the second heating does not modify the previous value of the susceptibility. As the first heating in the true Thellier method is made while the laboratory field is on, this method seems to be more adequate to detect CRM acquisition than the modified version by Coe [1967a] in which the first heating is made in zero field. Indeed, chemical alteration, in zero field, will not enable CRM acquisition.

The maximum temperature step which defines the linear part of the NRM-TRM diagram used to calculate the paleointensity is the last temperature step before any evidence of PTRM capacity changes. The linear segment defined in the NRM-TRM diagram where overprint and magnetochemical changes are negligible must contain at least four to five points and span no less than 15% of the total NRM in order to be reliable [Coe *et al.*, 1978, Prérot *et al.*, 1985b]. Special difficulties in the interpretation of the NRM-TRM appear when a curvature of the plot is observed along all the

temperature range, while no PTRM capacity alteration is observed. In this case, using the first part of the curve would result in overestimating the paleofield while the last part of the curve would give an underestimate of the paleointensity. This kind of curves can be explained if the magnetic carriers are multidomain grains [Levi, 1977] or if the NRM is not a pure TRM. The last hypothesis might be tested by comparing the blocking temperature spectrum and the Curie point [Prérot *et al.*, 1985b].

In our experiments, a minimum of 11 temperature steps were performed. The statistical method developed by Coe *et al.* [1978] was used to obtain the slope b of the straight line, its corresponding relative standard error σ_b and the standard error $\sigma(Fe)$ about the paleofield intensity Fe . The validity of the paleointensity determinations were expressed using the quality factor q estimated from the NRM fraction used f , the gap factor g and the scattering of the plot about the linear segment. An indication of the potential for error caused by CRM acquisition is given for each sample by the factor R , as defined by Coe *et al.* [1984]. It represents the maximum error, in percent of the laboratory field, that CRM would cause in the paleointensity estimate. Within a single volcanic unit, the average paleointensity was calculated using the weighting factor w , defined by Prérot *et al.* [1985b], the uncertainty about the mean was expressed by the standard deviation of the unweighted average.

Results

Paleointensity determinations were attempted on 48 samples, of which 26 have given reliable results on 11 distinct lava flows (Table 3).

Two types of non-ideal behavior occurred during the Thellier experiments. The first type is represented by samples for which the evolution in the PTRM capacity is indicated by negative PTRM checks. Sample PF37a is one example (Figure 12) for which a small overprint was cleaned at 250°C. While the first PTRM check at 380°C showed a decrease in the TRM acquisition capacity, all the following PTRM checks indicated an increase in the TRM capacity. Providing the PTRM checks have been carried out at several steps, this kind of behavior is easily recognized and no calculation of paleointensity can be attempted. In contrast, some samples provided concave up paleointensity curves with positive PTRM checks. Similar behavior has been found during the study of samples from the island of Huahine [Roperch and Duncan, this issue]. Samples showing important non-linearity in the paleointensity have been rejected.

More than half of our selected samples have provided reliable results. Most paleointensities are determined with 5 to 15 points, a NRM fraction typically close to 50%, and a quality factor q around 10. The highest temperatures used are generally close to the Curie point (near or above 500°C); this indicates a good thermal stability of the samples. The laboratory Koenigsberger ratio (Q_1) [Prérot *et al.*, 1985b] has been calculated for each sample, and the average value is 13.8, with a range from 5 to 63. The mean Q_1 is similar to the one obtained by Prérot *et al.* [1985b] in the most stable samples from Steens Mountain. Some paleointensity diagrams are shown in Figure 13 and results are summarized in Table 3 and Figure 14. On Figure 13, the demagnetization diagram of the NRM during the Thellier experiment is also shown. Because the NRM is determined while subtracting two opposite partial TRMs at each step, the very low noise observed on the orthogonal projections enhances the quality of these experiments.

Four paleointensity determinations have been obtained on two flows with reversed polarity; the flow R1N which precedes the Matuyama-Brunhes reversal and the flow BKB before the Cobb

Mountain transition. Only one experiment has been successful on one flow from the Jaramillo normal polarity subchron (flow CA). The results are close to the expected value at this latitude, from 27.1 to 54.3 μ T, and are in good agreement with those obtained in previous studies [Senanayake *et al.*, 1982].

Twenty-one paleointensity results from 8 distinct lava flows were obtained from 3 transitional zones: 14 paleointensity values from the Cobb Mountain transition (5 flows), 2 results from the Upper Jaramillo (1 flow) and 5 results from the Matuyama-Brunhes (2 flows). For the Cobb Mountain transition, the paleofields obtained are between 4 and 8.4 μ T. A lower value was obtained for the Upper Jaramillo transition with a field strength for the flow M2C of 2.6 μ T. The two flows from the Matuyama-Brunhes transition also give very low paleointensities, from 3.4 to 3.6 μ T. Good consistency between samples from the same flow is observed, except in the case of the flow BKK.

DISCUSSION

The Cobb Mountain event: Excursion or short normal polarity event?

An apparent R-T-R excursion of the Earth's magnetic field, dated around 1.1 Ma, is recorded in the volcanic sequence from Tahiti. Several paleomagnetic reports from marine or terrestrial sediments and volcanic rocks have suggested that a complete reversal of polarity occurred at that time but this event has not yet been classified in the main polarity time scales [Mankinen and Dalrymple, 1979; Harland *et al.*, 1982]. Therefore, a review of available data appears to be necessary.

The study of marine magnetic anomalies has enabled the recognition of the main features of the polarity sequence but short events with time duration of the order of 10,000 years are difficult to distinguish. On half of 14 magnetic profiles from a survey over the east Pacific Rise Crest, Rea and Blakely [1975] have identified a small positive magnetic anomaly centered around 1.1 Ma. They argued that the identification of this short magnetic anomaly as a geomagnetic event was only tentative, because this brief period of normal polarity did not show up well in their average profile.

Magnetostratigraphic studies of marine sediment cores and Pliocene continental deposits have, in some cases, revealed the existence of a short event before the Jaramillo subchron. But discontinuous sampling of cores as well as the time-averaging process in the acquisition of the magnetic remanence have made recognition of short period events difficult. An anomalous change in inclination before the Jaramillo normal subchron was found in one marine sediment core from the north Pacific [Ninkovich *et al.*, 1966] and transitional directions were reported from two cores of deep-sea calcareous sediments from the Melanesian basin [Kawai *et al.*, 1977; Sueishi *et al.*, 1979]. In this last case, the excursion has been dated at 1.06 Ma, extrapolated from the depth of the major boundaries of polarity epochs and the sedimentation rate. A complete reversal was suggested in one deep-sea core from the equatorial Pacific [Forster and Opdyke, 1970] and four cores from the Southern Ocean [Watkins, 1968], from which the normal polarity zone was dated around 1.07 Ma.

Kochegura and Zubakov [1978] summarized the results of their magnetostratigraphic studies of the marine and loess deposits of the Ponto-Caspian zone of USSR, and showed a normal polarity period just before the Jaramillo, occurring around 1.1 Ma, but no information on their paleomagnetic data were presented, making the quality of these results difficult to assess.

More recently, in the vicinity of the magnetozone correlated to the Jaramillo, several intervals of anomalous directions of

TABLE 3. Paleointensity Results

Sample	<i>D</i>	<i>I</i>	Js-T	Tc	<i>n</i>	<i>H_{lab}</i>	<i>J_{NRM}</i>	ΔT	<i>f</i>	<i>g</i>	<i>q</i>	<i>r</i>	R%	Fe $\pm\sigma$ Fe	Fe \pm s.d.	$\langle F_E \rangle$
R1N85	180.0	37.2	1a	531	15	34	18.8	200-570	0.899	0.891	40.8	0.997	2.6	38.8 \pm 0.8		
R1N84	181.1	36.7	1a	562	10	34	12.8	200-530	0.768	0.820	29.5	0.998	2.9	36.6 \pm 0.8	37.7 \pm 1.6	37.7
R1U128	237.5	9.0	1a	522	5	9	1.2	370-500	0.434	0.674	8.3	0.998	1.7	3.6 \pm 0.1		
R1U127	231.0	8.5	1b	527	6	9	1.1	330-500	0.406	0.738	21.7	0.999	4.3	3.3 \pm 0.1	3.4 \pm 0.2	3.4
TR067	230.0	0.0	1c	524	14	10	0.3	250-540	0.852	0.909	30.6	0.996	2.8	3.2 \pm 0.1		
TR068	229.6	4.7	1a	520	7	20	0.4	350-495	0.328	0.819	4.5	0.991	5.3	3.7 \pm 0.2		
TS063	230.8	5.7	1a	560	11	20	0.8	200-505	0.170	0.829	1.8	0.971	28.6	3.8 \pm 0.3	3.6 \pm 0.3	3.3
CA084	14.0	-26.7	1b	565	9	34	3.5	200-515	0.582	0.857	11.5	0.993	11.9	54.3 \pm 2.4		54.3
M2C52	205.0	51.0	N.d	N.d	12	10	0.4	300-540	0.829	0.883	30.5	0.997	2.4	2.6 \pm 0.1		
M2C54	210.0	61.0	N.d	N.d	7	15	0.6	300-480	0.242	0.800	3.1	0.990	7.8	2.5 \pm 0.2	2.6 \pm 0.1	2.6
BKT170	345.0	56.0	1c	527	8	10	1.1	350-500	0.422	0.784	8.8	0.996	11.05	4.0 \pm 0.2		4.0
PKC16	222.7	11.8	1c	522	11	20	2.0	350-535	0.601	0.863	16.7	0.996	4.6	6.6 \pm 0.2		
PKC17	218.3	10.5	1a	531	13	10	2.0	200-520	0.667	0.867	15.1	0.992	12.0	6.2 \pm 0.2		
PKC18	225.8	8.1	1a	533	11	20	2.2	350-535	0.623	0.866	14.1	0.993	3.5	6.2 \pm 0.2	6.3 \pm 0.2	6.3
BK197	158.5	-42.6	1a	531	11	20	2.3	350-535	0.518	0.880	9.4	0.990	4.6	6.6 \pm 0.3		
BK198	154.5	-44.1	1a	513	12	20	2.4	200-515	0.386	0.871	9.8	0.994	7.7	8.0 \pm 0.3		
BK199	158.0	-37.0	1a	542	9	10	1.0	350-510	0.495	0.841	5.2	0.977	14.1	8.7 \pm 0.7		
BK1100	148.2	-36.5	N.d	N.d	7	10	1.1	410-510	0.385	0.808	3.1	0.975	24.4	8.2 \pm 0.8	7.9 \pm 0.9	7.7
BKP147	346.5	29.2	N.d	N.d	13	9	0.8	200-550	0.738	0.867	23.6	0.996	18.0	9.0 \pm 0.2		
BKP144	348.0	27.6	N.d	N.d	10	9	0.8	200-530	0.558	0.870	12.8	0.994	13.5	8.7 \pm 0.3		
BKP148	347.8	25.1	1a	565	9	9	0.8	270-530	0.654	0.841	12.1	0.993	7.0	7.9 \pm 0.4		
BKP143	345.9	27.9	N.d	N.d	9	9	0.6	200-515	0.477	0.863	4.8	0.975	18.7	6.9 \pm 0.6	8.1 \pm 1.0	8.4
BKK114	224.4	-8.0	N.d	N.d	8	9	1.0	200-500	0.360	0.843	5.1	0.989	2.9	9.1 \pm 0.5		
BKK113	223.7	1.2	1c	511	11	10	0.8	250-510	0.468	0.840	8.1	0.989	3.2	3.9 \pm 0.2	6.5 \pm 3.7	6.1
BKB52	182.4	12.7	1a	550	9	34	4.5	200-510	0.469	0.835	8.4	0.992	10.4	28.5 \pm 1.3		
BKB47	182.5	8.5	1a	550	11	20	3.9	250-515	0.232	0.873	10.7	0.998	18.5	27.4 \pm 0.5	27.9 \pm 0.8	27.9

D and *I*, magnetic declination and inclination of the NRM left in the ΔT interval; Js-T, type of the thermomagnetic curve (N.d, not determined); Tc, Curie temperature of the sample; *n*, number of points in the ΔT interval; *H_{lab}*, intensity of the laboratory field in μT ; *J_{NRM}*, intensity of the natural remanence in Am^{-1} ; ΔT , interval of temperature used to determine the paleointensity; *f*, NRM fraction; *g*, gap factor; *q*, quality factor (*f, g, q* were defined by *Coe et al.*, 1978); *r*, linear correlation coefficient; R%, maximum percentage of CRM; Fe, paleointensity estimate for individual specimen in μT ; $\sigma(Fe)$, standard error; F_E , unweighted average paleointensity of individual lava flow in μT , plus or minus its standard deviation; $\langle F_E \rangle$, weighted mean in μT .

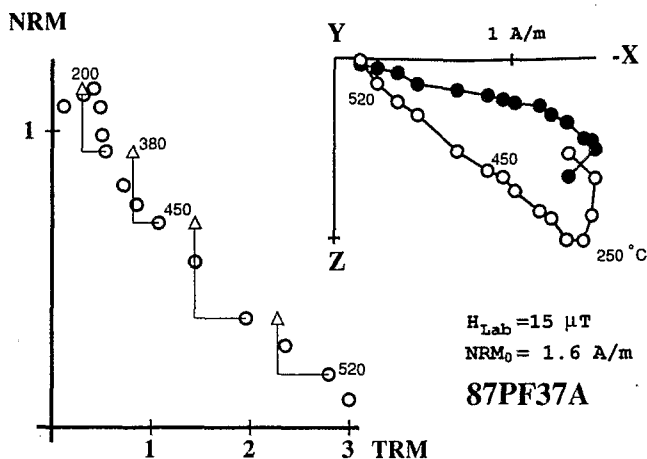


Fig. 12. NRM-TRM diagrams, normalized to the initial NRM (NRM_0), showing non-ideal behavior during paleointensity determination. Orthogonal plots in sample coordinates represent the evolution of the remanent vector during the experiment. H_{Lab} : intensity of the laboratory field in μT . Sample 87PF37A shows negative PTRM checks indicating that magnetic alteration occurred during the experiment.

magnetization have been observed in deep-sea cores from the Caribbean DSDP Site 502 [Kent and Spariosu, 1982]. The most detailed record of an event of normal polarity preceding the Jaramillo subchron was obtained from sediment cores from the north Atlantic [Clement and Kent, 1986]. In this study, the event has been dated around 1.16 Ma, assuming a constant sedimentation rate between the depths of the the major polarity chrons, and its time duration was estimated to be 11,600 years. Nevertheless, the normal period in this record is disrupted by very shallow inclinations and the authors argue that the proximity of this large directional swing to the upper transitional zone, and the occurrence within an intensity minima, suggest that they are part of the transitional behavior. Thus, the true normal period might be as short as 5,000 years.

Some normal or intermediate directions have also been found, in several places, on volcanic flows dated around 1.1 Ma., but the imprecision in radiometric dating was often great enough to allow the possibility that they cooled within the Jaramillo subchron.

The name Cobb Mountain was given by Mankinen et al. [1978] to an event which, for the first time, was found in a volcanic unit, a composite rhyolite and dacite dome, situated in northern California. K-Ar datings have given a mean age of 1.12 ± 0.02 Ma. Transitional directions were clearly recorded in 5 sites of rhyolites, while the normal polarity was defined only by a strong normal overprint at one particular locality, where the rock is completely devitrified. Because no evidence of late hydrothermal alteration was found on the Cobb Mountain, Mankinen et al. argued that this devitrification was caused by deuteric alteration which could have started shortly after eruption. Therefore the NRM direction was considered as representing a complete change from intermediate to normal polarity during the cooling of the rhyolite.

One intermediate polarity lava flow dated by K-Ar at 1.13 ± 0.08 Ma and six flows with a normal polarity with age from 1.07 to 1.37 Ma have been reported by Briden et al. [1979] in a study of volcanic rocks from the islands of St. Vincent and La Guadeloupe, in the Lesser Antilles. On the island of Madeira, one normally magnetized basalt dated at 1.15 Ma has been found by Watkins and Abdel-Monem [1971]. Using the new constants in K-Ar datings [Mankinen and Dalrymple, 1979], this age became 1.18 Ma. Two basalt flows in the Coso Range, California with a

normal polarity have given an age about 1.08 Ma, close to the previous one obtained on the Cobb Mountain [Mankinen and Grommé, 1982]. However the age uncertainties are quite large for these two flows (about 12%). Normal polarities from volcanic units with ages around 1.05 Ma have also been reported by Fleck et al. [1972] in south Argentina, Abdel-Monem et al. [1972] on the island of Tenerife and McDougall and Chamalaun [1966] in the island of La Réunion. However it should be noted that no information concerning the polarity of the flows above and below was available. Thus, the interpretation must rely strictly on the K-Ar results. A normal polarity period, preceding the Jaramillo, was found in an ash layer and adjacent sediments from the deposits of the Osaka group (Japan) [Maenaka, 1979]. The ash horizon has given a fission track age of 1.1 ± 0.01 Ma. The use of only one level of AF cleaning might have not been sufficient to remove a possible strong normal overprint.

This review shows the difficulty in identifying a short geomagnetic event either in sediment or volcanic units. However, there is now strong evidence for a worldwide geomagnetic feature of either a short event or an excursion around 1.1 Ma. Our data from the Punaruu valley suggest that the field did not reach a full normal polarity. Nevertheless, the detailed record from core 609b [Clement and Kent, 1987] suggests a very short time for the normal period. Therefore, such a short normal polarity might correspond to a hiatus in the volcanic activity at that time and only the transitional boundaries were recorded.

Comparison of the transitional field characteristics with other available records

A comparison of the intermediate states of the field observed at different sites for a single reversal may provide a clue to the understanding of the reversal process. To do that, a review of the other records is necessary.

The Cobb Mountain. As discussed before, the most detailed record concerning the Cobb Mountain event was reported from hydraulic piston cored sediments by Clement and Kent [1987]. This record has one main characteristic in that while the declination exhibits very short transition for both the onset and the termination of the normal polarity period, large variations in inclination occur before and after the declination changes. As noted earlier an important shallowing of the inclination is also reported in the normal polarity period as defined with the declination pattern by Clement and Kent [1987]. The VGPs associated with these intermediate directions are almost confined in the meridian plane containing the site and show a well defined antisymmetry between the onset and the termination.

In the record from French Polynesia, we observed three different groups of intermediate directions. Obviously, they represent only a few snapshots of an excursion, or limited records of one or both transitions limiting an undetected normal polarity event. Reliable paleointensities have been obtained for these flows with fields from 4 to 8 μT . There is no evidence for a strong intermediate state. Accepting that these flows record an excursion, the magnetic data show that the intermediate field during the Cobb Mountain had similar characteristics to those observed during polarity reversals, supporting the interpretation of excursions as aborted reversals [Hoffman, 1981b].

Lower and Upper Jaramillo. Up to now, deep-sea sedimentary core records of the transitions delimiting the Jaramillo have been obtained in the Indian Ocean [Opdyke et al., 1973, Clement and Kent, 1984, 1985], in the north Atlantic Ocean [Clement and Kent, 1986] and Pacific Ocean [Hammond et al., 1979; Herrero-Bervera and Theyer, 1986, Theyer et al., 1985]. From volcanic

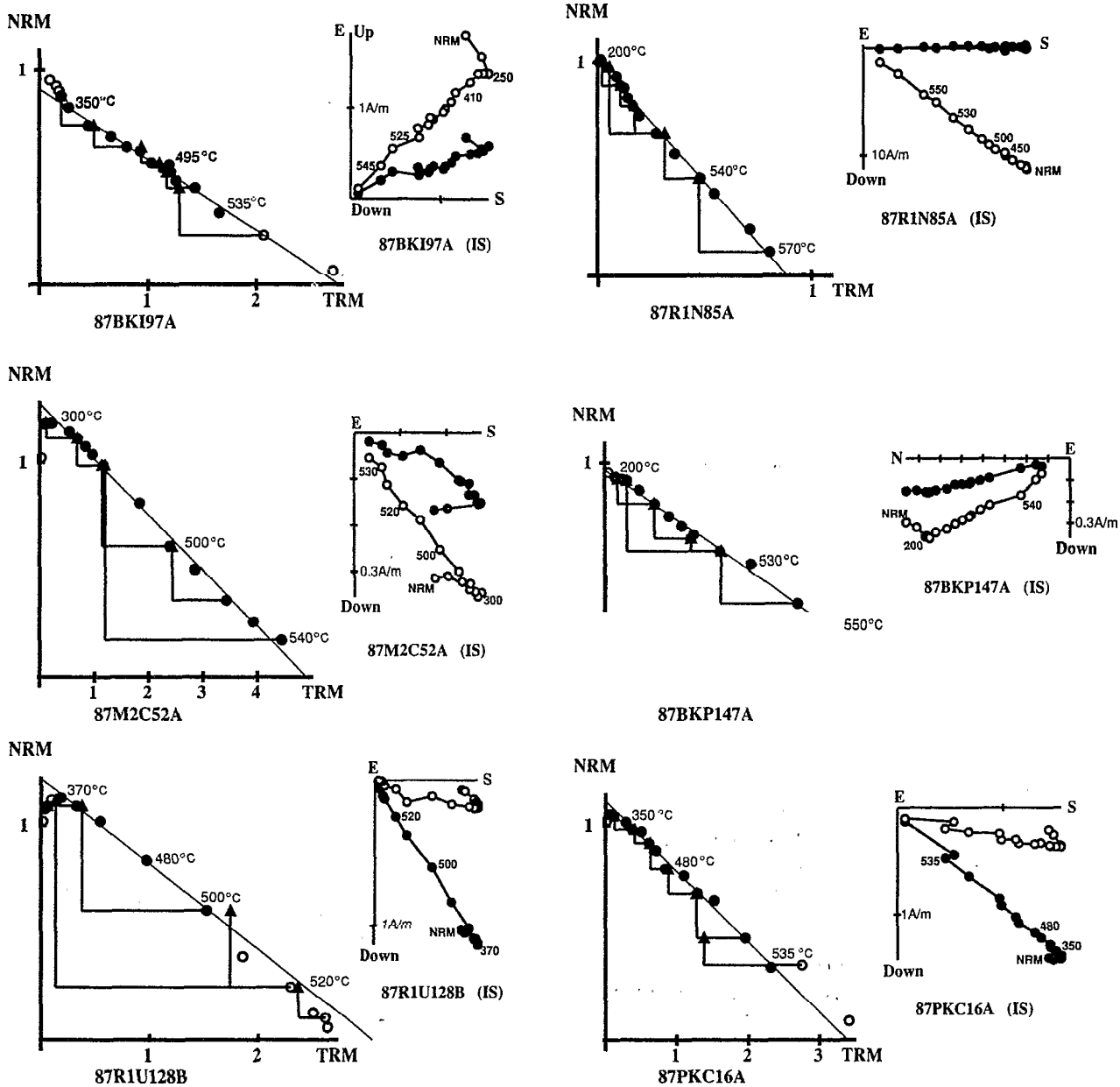


Fig. 13. NRM-TRM diagrams of accurate paleointensity determinations using a large portion of the NRM. The orthogonal plots show the evolution of the remanent vector in geographical (in situ) coordinates.

records, a few intermediate directions come from the study of *Mankinen et al.* [1981] on Clear Lake (California).

Data from deep-sea cores from the Pacific Ocean are, in our opinion, difficult to interpret, simply because of the very low sedimentation rates, as low as $6 \text{ mm}/10^3 \text{ years}$ [*Hammond et al.*, 1979] or $7.8 \text{ mm}/10^3 \text{ years}$ [*Theyer et al.*, 1985]. If the remanence is a detrital remanent magnetization (DRM), each sample, no matter how closely spaced, represents an average of the paleomagnetic signal over a great period of time; in the case of a PDRM (post-DRM), the transition can be completely missed or the directions observed can differ completely from the true configuration of the intermediate geomagnetic field [*Valet*, 1985; *Hoffman and Slade*, 1986]. Records of the lower Jaramillo from terrestrial sediments were described by *Gurarii* [1981], from the territory of western Turkmenia (USSR) but, since the remanence is carried by two magnetic minerals, hematite and magnetite, the nature of the magnetic remanence (detrital and chemical) is unclear.

The important shallowing of the inclination seen at the beginning of the lower Jaramillo record from the Indian Ocean [*Clement and Kent*, 1984] clearly disagrees with the observation from Tahiti, in terms of a simple zonal harmonic model.

Herrero-Bervera and Theyer [1986] have presented a non-axisymmetric behavior of the field during the upper Jaramillo recorded by deep-sea sediments from a site near Hawaii (sedimentation rate $35 \text{ mm}/10^3 \text{ years}$). This record is mostly characterized by oscillations between reverse and normal polarities. This behavior may question the possibility that antipodal magnetizations are present in the samples. Assuming that this record is reliable leads to the conclusion that transitional fields recorded at a site at a low northern latitude in the same longitudinal band as the Society islands have no common features with those recorded at Tahiti.

The record of the Upper Jaramillo transition in deep-sea sediments from the Indian Ocean shows evidence of bioturbation,

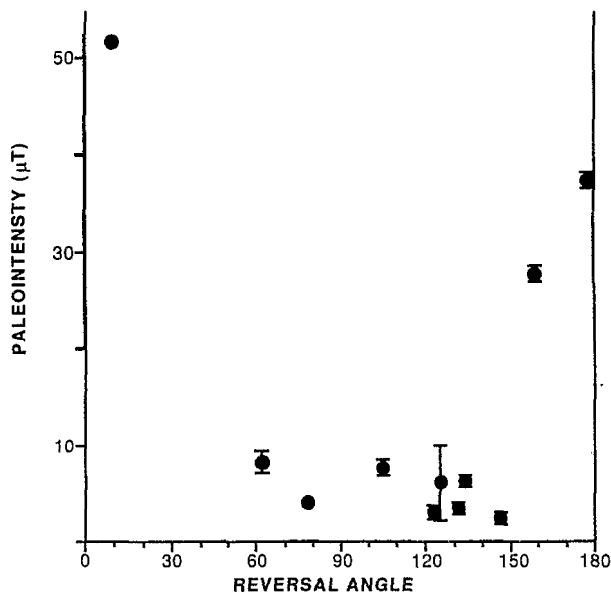


Fig. 14. Diagram showing the evolution of the mean paleointensities per flow with their standard deviations, versus the angular departure from the axial normal dipole. Paleointensities obtained from the intermediate flows are below $10 \mu\text{T}$.

which might well have acted to smooth the transition [Opdyke *et al.*, 1973; Clement and Kent, 1985]. The sediments from the north Atlantic ocean [Clement and Kent, 1986], which are characterized by a sedimentation rate of $82 \text{ mm}/10^3 \text{ years}$, have given a record of the Upper Jaramillo in which full normal polarity directions are not observed at the base of the sampling zone, and therefore the lower boundary of the transition is not defined. Moreover, this record displays strong variations in intensity of magnetization which are apparently correlated to changes in the lithology.

So we are faced with the disappointing conclusion that no fully reliable data are available for comparison with our detailed record from the Upper Jaramillo. Only one accurate paleointensity was obtained for the Upper Jaramillo transition (Table 3) showing a field strength close to $2.6 \mu\text{T}$, but all the NRM intensity data indicate that the intensity of the field might have been particularly low during this reversal. As was already pointed out, an intermediate direction associated with a low NRM intensity was observed in flow R1D which follows the Jaramillo transition termination. This direction has an angular departure of almost 40° from the full reversed polarity. This is not the first time that a brief polarity fluctuation is described close to that polarity boundary. Clement and Kent [1986] observed a 60° swing in the inclination just after the upper Jaramillo transition. In the lava flows of Clear Lake (California) [Mankinen *et al.*, 1981] a sequence of intermediate polarity lavas, apparently younger than reversed lavas above the Jaramillo termination, has been found. The K-Ar age obtained on one of the intermediate flows ($0.90 \pm 0.02 \text{ Ma}$) is indistinguishable from the age of the end of the upper Jaramillo transition, suggesting that the brief intermediate state observed is part of the reversal boundary, and represents what is generally called a rebound effect [Prévot *et al.*, 1985b; Laj *et al.*, 1987, 1988]. Our data from flow R1D can be interpreted in this way. On the other hand, some data from Clear Lake and deep-sea sediments from the Southern Ocean [Watkins, 1968], suggest that a polarity event might also have occurred at about $0.83\text{--}0.85 \text{ Ma}$, which could also explain the direction of flow R1D. Without an estimate of the age of this flow, we cannot choose between these two possibilities.

Matuyama-Brunhes. This transition is poorly defined but at least for the limited part of the transition recorded in the Tahiti section, there is convincing evidence that the field was low ($3\text{--}4 \mu\text{T}$).

There are many sedimentary records of this reversal. A strong dependence of the VGP path during the reversal with the longitude of the observation sites was first pointed out by Fuller *et al.* [1979]. However, careful examination of the data convinced us that some sediments have not accurately recorded the weak geomagnetic field and that the geometry of the transitional field might not be as simple as recently proposed by Hoffman [1988]. In the case of the Japanese record [Niitsuma *et al.*, 1971], the NRM intensity data are scattered and no clear variation of the intensity can be observed. With sediments from the mid-northern and equatorial Pacific [Clement *et al.*, 1982], dissimilar VGP paths have been obtained from two nearby cores, and an increased dispersion in directions was observed within the transitional zone. These observations suggested to Clement *et al.* that some sedimentological factors have probably distorted the magnetization of these sediments characterized by a low sedimentation rate ($7 \text{ to } 11 \text{ mm}/10^3 \text{ years}$).

The accuracy of some paleomagnetic techniques to clearly isolate the primary remanent direction (if it still exists and has not been replaced by subsequent geochemical processes [Karlin *et al.*, 1987]) constitutes one of the major problems. The lake Tecopa record [Hillhouse and Cox, 1976] has been long considered one of the most reliable records of the last polarity reversal. However, a resampling of the section and new data obtained by thermal demagnetization [Valet *et al.*, 1988a] shows clearly that strong magnetic overprints are not removed by AF demagnetizations. The previously reported intermediate directions were the result of a superimposition of reverse and normal components of magnetization, and provide no useful information about the reversal. Although Valet *et al.* [1988a] showed that AF demagnetization did not isolate a primary component, they did not demonstrate in a convincing manner that the intermediate directions isolated by thermal demagnetization are meaningful.

Recently, data from the equatorial Atlantic Ocean (Site 664) have been reported from deep-sea sedimentary cores [Valet *et al.*, 1989]. In comparing the VGP path they obtained with deep-sea core results from a site of the same longitude (Site 609), but situated at a mid-northern latitude [Clement and Kent, 1986], Valet *et al.* [1989] showed that the two records provide antipodal VGP paths, located over America (Site 609) and Asia (Site 664), a fact that cannot be reconciled with a simple axial geometry of the transitional field. Obviously, even for this 'well' documented reversal, a close look at the data shows that still more accurate paleomagnetic records are needed for a better description of the transitional field.

The second part of this discussion will include some of the results obtained on the island of Huahine [Roperch and Duncan, this issue].

Zonal and non-zonal components

East and west intermediate directions are more numerous in the record of the N-T-N excursion of Huahine than in the records from Tahiti which show smaller deviations from the north/south vertical plane. On average, non-zonal components are as important as the components lying within the geographical meridian during transitions, as suggested by Prévot *et al.* [1985b] for the Steens Mountain record. However, data from Polynesia may indicate two different configurations for the beginning and the middle of the reversal. For the lower Jaramillo at Tahiti and the beginning of the transition from Huahine, there is some evidence for axisymmetry

characterized by a path through high inclinations (Figure 15). *Roperch and Duncan* [this issue] suggest that this simple apparent structure can be modeled with a growing zonal quadrupole of the same sign as the decaying dipole. The evidence, from Polynesia, for a quadrupole field at the onset of a reversal is in agreement with the prediction made by *Merrill and McFadden* [1988] who have argued that a reversal may occur if the axial dipole field is weak and the quadrupole family field is strong.

Variation in the geomagnetic field intensity

Intensity of the NRM versus directions or VGPs. As we discussed earlier, the NRM intensities (at 10 mT) can reflect the average variations in the geomagnetic field intensity. All the NRM intensity data from Huahine and Tahiti have been grouped by 10° intervals in reversal angles and VGP latitudes; then, arithmetic and geometric mean values were calculated for each group (Figures 16a, b). The standard error bars have been reported for the

arithmetic means. Differences between arithmetic and geometric averages underline the scatter in each data set. As the NRM intensity depends on the strength of the geomagnetic field and the magnetic mineralogy of rocks, it seems reasonable to simply add the two data sets from Huahine and Tahiti. Indeed, these data are from the same geographical area and the volcanic rocks which form these two islands have similar compositions. The average values, within each reversal angle group, of the NRM data for Tahiti, Huahine and for the combined data sets are reported in Table 4. In combining the two data sets the number of sites used is quite large (220), and we assume that short-term field paleointensity variations and NRM intensity fluctuations due to rock magnetic properties have been averaged. An important drop in intensity is observed for reversal angles from 0° to 30° or VGP latitudes from 90° to 60°. For higher reversal angles (i.e., lower VGP latitudes) the intensities stay very low, around 1 A/m or less. The same result is obtained using either the data from Huahine or Tahiti,

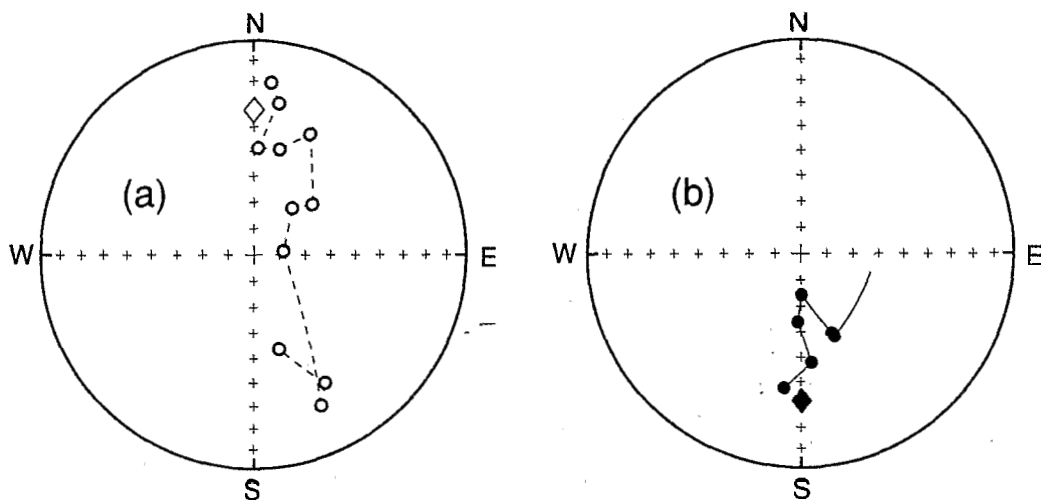


Fig. 15. Equal area projections of paleomagnetic directions observed at the beginning of the N-N Huahine excursion (a) and the lower Jaramillo transition (b) recorded at Tahiti. In these two cases, the directions go through high inclinations leading us to suggest that the beginning of a transition might be controlled by axisymmetric components of the field.

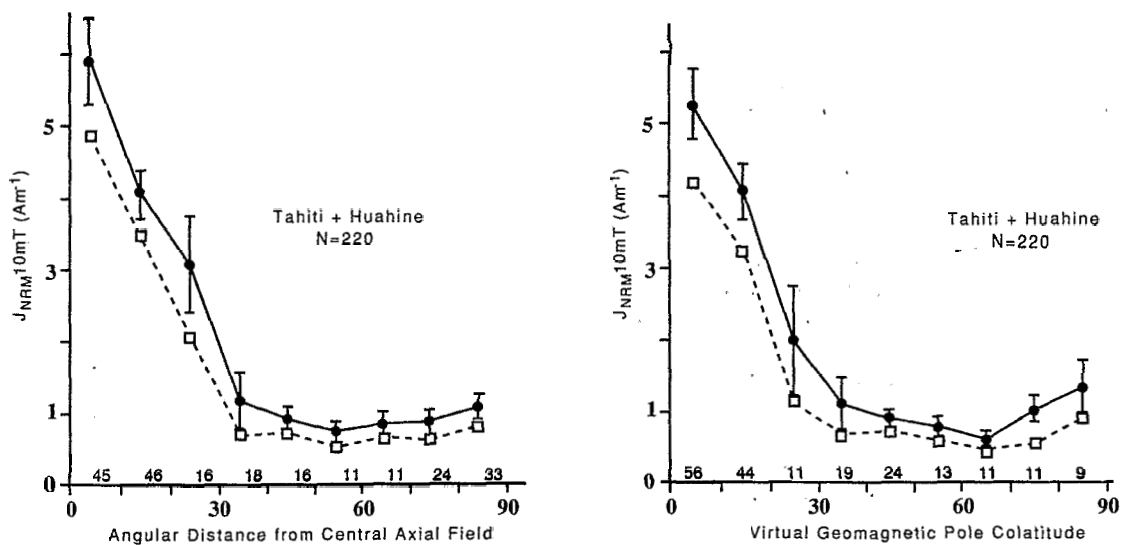


Fig. 16. Diagrams showing the variations of the mean NRM intensity (after 10 mT) averaged for group of flows from Polynesia, versus the angular departure from central axial field (A) or versus virtual geomagnetic pole latitude (B). The reversed directions have been inverted and added to the normal ones. The arithmetic means (black dots) are shown with their standard error bars while open circles refer to geometric means. The number of sites available in each interval is also indicated.

TABLE 4. Average NRM Intensities

δ (°)	Tahiti			Huahine			Tahiti+Huahine		
	N	J_n	err	N	J_n	err	N	J_n	err
10	29	4.9	0.97	16	4.8	0.49	45	4.8	0.64
20	34	3.7	0.43	12	2.8	0.57	46	3.5	0.35
30	11	2.6	0.94	5	1.2	0.65	16	2.0	0.71
40	3	0.8	0.77	15	0.7	0.48	18	0.7	0.41
50	11	0.7	0.13	5	0.9	0.35	16	0.7	0.14
60	7	0.6	0.13	4	0.5	0.42	11	0.6	0.16
70	6	0.5	0.09	5	1.1	0.23	11	0.7	0.15
80	10	0.4	0.16	14	0.7	0.24	24	0.6	0.16
90	8	0.6	0.13	25	0.8	0.21	33	0.8	0.16

N , number of sites; J_n , geometric mean of NRM intensities in Am^{-1} (at 10 mT), by 10° intervals in reversal angles (δ); *err*, standard error.

giving us some confidence in the observed distribution. This behavior in the NRM intensities suggests that for reversal angles higher than 30° the geomagnetic field is purely transitional at this latitude, and that the mean intensity of the field stays very weak during the entire transitional period. However, we must emphasize that this representation enables only the recognition of average field variations and these values do not, for example, show what was the maximum intensity reached during the transitions.

A similar study has been reported for a data set of more than two thousand lava flows from Iceland by *Kristjansson and McDougall* [1982] and *Kristjansson* [1985]. Comparison of results from these two sites at different latitudes deserves consideration. For this reason, both geometric mean values have been normalized by the intensity observed within the 0 - 10° interval in reversal angles or VGP colatitudes (Figure-17). With respect to the deviations from the axial dipole direction, the decrease in intensity observed in Polynesia is also observed in Iceland with a cut-off level between transitional and stable period around 30° to 40° departure from the central axial dipole. On average, however, the intensity of the transitional geomagnetic field appears to have been

higher in Iceland than at a low latitude site like Polynesia; the ratio of the transitional field to stable period intensities might be around 25-30% in Iceland and 10-20% in Polynesia. As the intensity of the normal and reversed field is higher in Iceland than in Polynesia, this indicates significant differences between the average paleointensity during transitions between these two sites. These data may suggest a latitudinal dependence of intermediate fields. It is interesting to note that one well established feature of paleosecular variation is the increase of the scatter of VGPs with increase in latitude.

While in Polynesia the decrease of the relative mean intensity with decreasing VGP latitude is similar to that defined with directions, the drop in intensity with VGP colatitude is particularly smooth in Iceland. The dipole wobble is not large as seen from Polynesia and the smooth variation observed in Iceland might result from the VGP calculation process because of a stronger non-dipole field.

Because the average field during periods just before and after the reversal may not be representative of the average field during longer stable periods, such as a chron or a subchron, a bias is perhaps introduced in our data. Indeed, a great percentage of measured flows sampled transitional zones, especially in the case of Huahine, while the sampling in Tahiti is more regular and covers an interval of time around 0.6 Ma. Our data set is about ten times less than the one from Iceland, however, and this can explain the quite large error bars observed in some cases. Certainly, additional data from different sites are needed to better constrain our present observations and our interpretations.

Absolute paleointensities during reversals. Our absolute paleointensity data range from 2 to $8\mu\text{T}$ with an average around 5-6 μT . More determinations are still needed, but it seems that our paleointensities are significantly lower than the average intensity during the Steens Mountains transition, which is close to 11 μT [*Prévot et al.*, 1985a]. In view of the paleointensity determinations, and the variations in the NRM intensities with angular departures from the central axial dipole, it seems that the average intensity of the field during transitions might be

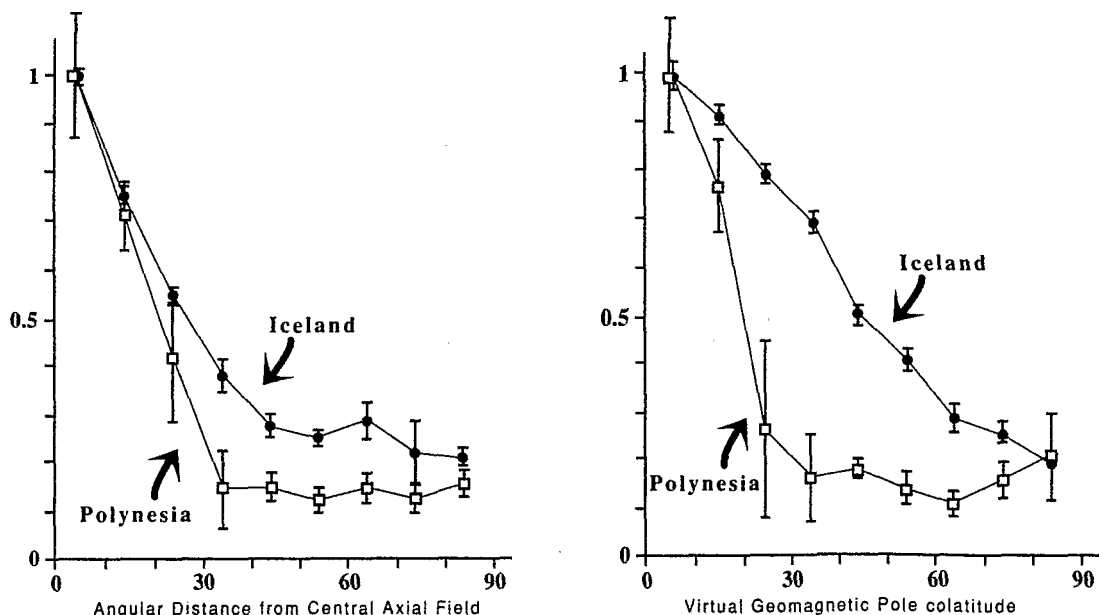


Fig. 17. Comparison of the variations of the average geometric mean values of intensity of magnetization (after 10 mT) from Polynesia and Iceland versus the reversal angle and the VGP latitudes. Data from Iceland are extracted from *Kristjansson* [1985]. In order to enable comparison, each data set has been normalized to their respective first value in the 0 - 10° interval. The arithmetic standard errors have also been normalized.

latitudinally dependent, with possibly higher values at high latitudes than at low latitudes, in contrast to what was suggested by Prévot *et al.* [1985a].

On the other hand, few data from studies of reversals in Hawaii [Bogue and Coe, 1984] and from three excursions recorded by lava of Oahu [Coe *et al.*, 1984] indicate stronger paleointensities than those observed in Polynesia. Obviously, the small amount of accurate data that is available limits the discussion. Shaw [1975, 1977] reported high paleointensities during transitions while Lawley [1970] indicated weak field (about 5 μT) during Neogene polarity transitions recorded in Iceland, but obviously results obtained by total TRM methods are questionable because they may give erroneous results if thermal alterations of the samples are not detected. Very low intensities of the field, as low as 3 μT have some important implications. With such low magnetic vectors, large variations in direction may occur more easily than with a strong field because they do not correspond to large total vector changes.

Alteration of the geomagnetic signal by the recording medium

It is well known that the irregular extrusion rate of lava flows and the smoothing processes in sediments and intrusion may alter significantly the record of geomagnetic reversal paths [Weeks *et al.*, 1988]. However, we must emphasize that volcanic rocks record accurately the magnetic field even if providing only incomplete and intermittent records of a reversal. On the contrary, Hoffman and Slade [1986] demonstrated that smoothing effects in sedimentary records may provide reversal features with no relation to the geomagnetic field. Other problems attend interpretation of magnetic field variations from paleomagnetic vectors, particularly when records of low intensity fields may be damaged by any kind of local perturbations. For example, the local crustal magnetic anomaly may be significant. The intensity of the magnetic anomaly developed by an island like Tahiti remains very low compared to the strength of the geomagnetic field during normal or reversed periods. Giving an average remanent intensity to the volcanic rocks between 5 to 10 A/m, a homogeneous volcanic cone of the size of Tahiti can develop, at its surface, a local magnetic field between 0.5 to 1 μT , which are low values. The magnetization induced by the Earth's field is negligible in view of our Koenigsberger ratios; this is particularly true when the field intensity is already low. This means that during a transition, with a geomagnetic field close to 3 μT , at least two-thirds of the recorded magnetic field is of internal geomagnetic origin. Obviously, because magnetic anomalies have strong dependence with the shape of the body, short wavelength variations could exist. In the case of our data, we do not think that local effects play a major role because similar directions were recorded several hundreds meters apart.

We do not know what the implications are of such low paleointensities for the complicated processes of remanence acquisition in sedimentary rocks. One can speculate that it would be difficult for a sediment to adequately record a transition when the magnetic strength needed to align grains becomes too weak. Thus, some sediments may not be able to record the middle part of a transition but only the beginning and the end of a transition when the field decays or grows toward the other polarity. The fact that several records [Clement and Kent, 1984; Valet *et al.*, 1988b] have a shallow inclination in the middle of the reversal may indicate that the sedimentary process may control the remanence in some cases. A typical example might be the Lower Jaramillo record from a southern hemisphere core [Clement and Kent, 1984] which is marked by a regular shallowing of the inclination while the noise level in declination appears to slightly increase.

Implications for and from theoretical studies

Recently, a new interest in the reversal process has been triggered by the development of models which seem sufficiently specific to be tested against the paleomagnetic data. Combining detailed studies of the recent field and inversion methods, Bloxham and Gubbins [1985] have produced maps of the radial component of the field at the core-mantle boundary (CMB) from the years 1715 to 1980. Static features, associated with the main standing field generated by the dynamo, and rapidly drifting features are observed [Gubbins and Bloxham, 1987]. The development of reverse flux patches in the middle southern Atlantic hemisphere is possibly explained by expulsion of toroidal flux by fluid upwelling [Bloxham, 1986]. Gubbins [1987] suggested that the location of these reverse flux zones would be tied to mantle temperature anomalies, and that their growth provides a mechanism for polarity reversals. However, the large decrease of the paleointensity during reversals is one of the best established characteristics which suggests a general breakdown of the dipole. Thus, the growing of one reverse flux zone may not systematically provide low intensities everywhere.

This model predicts also that all reversals should be similar (i.e., have the same transitional field) within the life-time of the mantle convection pattern. Some sedimentary records seem to provide negative evidence for this model [Laj *et al.*, 1988], even if there are indications in records from Crete that the reversal process may remain invariant over several polarity intervals [Valet and Laj, 1984]. Different transitions from Polynesia exhibit some common features. In particular, southwest directions with shallow inclination are observed in 4 out of 5 transition records, but it is not obvious that such correlations are significant.

Comparing his theory with available paleomagnetic data, Gubbins [1988] argued that reverse flux features have been absent within the northern hemisphere since 5 Ma. This idea of a constant region where reversals are initiated is quite equivalent to the common starting point for a reversal model of the type suggested by Hoffman [1979]. Comparing our results with data from the Indian Ocean area would be helpful in constraining Gubbins's model. Even if there is no clear paleomagnetic data supporting Gubbins's reversal scheme, there is now strong evidence that thermal and topographic variations at the core-mantle boundary are constraining field variations, particularly the long-term changes in the mean reversal rate [McFadden and Merrill, 1984; Courtillot and Besse, 1987].

Geomagnetic polarity reversals in a turbulent core were investigated theoretically by Olson [1983] using the α^2 dynamo model. Olson considered that changes in the sign of helicity in an α^2 dynamo can provide two types of reversals, 'component reversals' when only the poloidal or the toroidal field reverse, and 'full reversal' when the two field components reverse. Following Olson, reversals would be the result of the competition between two source powers of the dynamo: heat lost at the CMB and progressive crystallization of the solid inner core. Over a brief interval, the contribution from inner core growth may exceed the contribution from heat lost at the CMB, causing a transient reversal of helicity.

The mathematical analysis from Olson [1983] predicts the variation of the dipole intensity for a field reversal with a reasonable time duration, but it does not define the non-dipole configuration of the field during the transition. Clement [1987] used the dipole time evolution equations from Olson's theory and assumed that the energy lost by the dipole field is partitioned to low degree non-dipole fields [Williams and Fuller, 1981] for modeling records of two reversals from both northern and southern

hemispheres. The fit to the data is strongly dependent on the way the dipole energy is distributed to the other terms. The attempt made by *Clement* [1987] was not successful for matching the intensity pattern which should be the main parameter for a rigorous test of *Olson's* hypothesis on the variation of the dipole intensity. The two previous theories assume that polarity reversals result from disturbances perturbing the movement in the core which produce the stable main field. This hypothesis is in agreement with the conclusion of the analysis of the geomagnetic reversal sequence made by *McFadden and Merrill* [1986] which indicates that the triggering effect of reversal might be independent of the process producing the main field.

Our data show, like other volcanic records, that the intensity of the geomagnetic field at the Earth's surface is considerably reduced (one fifth to one tenth) during the transition. It seems reasonable to think that the field intensity is also reduced in the core and that the magnetic energy lost is transferred into kinematic energy [*Prérot et al.*, 1985a], increasing the level of turbulence within the liquid core. This effect has been suggested in order to explain the large and quick directional changes observed in some record of polarity reversal. In particular, the 'geomagnetic impulses' occurring during the Steens Mountain transition imply a rate of change of the field components considerably larger than the maximum rate calculated for the recent secular variation [*Prérot et al.*, 1985a]. Resampling of several flows and detailed thermal demagnetization associated with a cooling model of the lava flows, might indicate even quicker directional changes of the geomagnetic field [*Coe and Prérot*, 1989]. We have not found such behavior in our volcanic sequences.

CONCLUSIONS

Four transitional zones have been sampled in a volcanic sequence of 120 lava flows in one valley of the island of Tahiti. According to the radiometric dating, they correspond to the Cobb Mountain, the lower and upper Jaramillo and the Matuyama-Brunhes transitions.

Paleomagnetic data indicate that the Cobb Mountain record may correspond to a Reverse to Reverse excursion of the Earth's magnetic field, occurring around 1.1 Ma.

Combining data from the island of Tahiti with the record of a Normal to Normal excursion in lavas from the island of Huahine [*Roperch and Duncan*, this issue], the non-zonal components of the field appear important during the transition. Nevertheless, the beginning of two transitions (the lower Jaramillo and the N-N excursion from Huahine), seems to indicate that the onset of a reversal could be more axisymmetric than the following phase. An increase in intensity of the quadrupole field at the onset of the reversal may fit the observed high inclination path.

NRM intensity data show that the intensity of the transitional field, at this latitude was very low. This fact is confirmed by some reliable paleointensity determinations, which indicate a paleofield strength around 3 to 8 μT . Comparison between average NRM intensity from Iceland and Polynesia indicate a lower averaged transitional field at low latitude than at high latitude. The response of the different paleomagnetic recorders to such low and rapid changing fields needs to be investigated in order to select the most reliable paleomagnetic records of the transitional field.

The main features of a polarity transition, i.e., short duration, non-dipole configuration and large drop in intensity, are now well established. However, these characteristics provide little evidence for a clear understanding of the processes occurring in the Earth's liquid core which lead to geomagnetic reversals. Other reversal records with a better worldwide coverage of the same transition,

absolute paleointensities and a more critical judgment on the data quality are needed to clearly establish some other features of reversals of geomagnetic field (i.e. axisymmetry at the onset, latitudinal dependency of the intensity of the intermediate field, ultra rapid field variations), and to make further progress in the theoretical understanding of the reversal process.

Acknowledgments. Thanks are due to Leonard Chungue and the Centre ORSTOM of Tahiti for providing the logistical support for sample collecting. We are indebted to Dr. Talandier for his hospitality at the Laboratoire de Géophysique de Pamatai. Discussions with K.A. Hoffman, C. Laj and M. Prérot have been very helpful at different stages of this study.

REFERENCES

- Abdel-Monem, A., N.D. Watkins, and P.W. Gast, Potassium-Argon ages, volcanic stratigraphy and geomagnetic polarity history of the Canary islands: Tenerife, la Palma and Hierro, *Am. J. Sci.*, 272, 805-825, 1972.
- Bloxham, J., The expulsion of magnetic flux from the Earth's core, *Geophys. J. R. Astron. Soc.*, 87, 669-678, 1986.
- Bloxham, J., The dynamical regime of fluid flow at the core surface, *Geophys. Res. Lett.*, 15, 585-588, 1988.
- Bloxham, J., and D. Gubbins, The secular variation of earth's magnetic field, *Nature*, 317, 777-781, 1985.
- Bogue, S.W., and R.S. Coe, Transitional paleointensities from Kauai, Hawaii, and geomagnetic reversals models, *J. Geophys. Res.*, 89, 10341-10354, 1984.
- Briden, J.C., D.C. Rex, A.M. Faller, and J.F. Tromblin, K-Ar geochronology and palaeomagnetism of volcanic rocks in the lesser Antilles island arc, *Philos. Trans. R. Soc. London, Ser. A*, 291, 485-528, 1979.
- Clement, B.M., Paleomagnetic evidence of reversals resulting from helicity fluctuations in a turbulent core, *J. Geophys. Res.*, 92, 10629-10638, 1987.
- Clement, B.M., D.V. Kent, and N. Opdykē, Brunhes-Matuyama polarity transition in three deep-sea sediments cores, *Philos. Trans. R. Soc. London, Ser. A*, 306, 113-119, 1982.
- Clement, B.M., and D.V. Kent, A detailed record of the Lower Jaramillo polarity transition from the southern hemisphere, deep-sea sediments cores, *J. Geophys. Res.*, 89, 1049-1058, 1984.
- Clement, B.M., and D.V. Kent, A comparison of two sequential geomagnetic polarity transitions (Upper Olduvai and Lower Jaramillo) from the southern hemisphere, *Phys. Earth Planet. Inter.*, 39, 301-313, 1985.
- Clement, B.M. and D.V. Kent, Geomagnetic polarity transition records from five hydraulic piston core sites in the north Atlantic, *Initial. Rep. Deep Sea Drill. Proj.*, 94, 831-852, 1986.
- Clement, B.M. and D.V. Kent, Short polarity intervals within the Matuyama: Transitional field records from hydraulic piston cored sediments from the north Atlantic, *Earth Planet. Sci. Lett.*, 81, 253-264, 1987.
- Coe, R.S., Paleointensities of the Earth's magnetic field determined from Tertiary and Quaternary rocks, *J. Geophys. Res.*, 72, 3247-3262, 1967a.
- Coe, R.S., The determination of paleointensities of the Earth's magnetic field with emphasis on mechanisms which could cause non-ideal behavior in Thellier's method, *J. Geomagn. Geoelectr.*, 19, 157-179, 1967b.
- Coe, R.S., and C.S. Grommé, A comparison of three methods of determining geomagnetic paleointensities, *J. Geomagn. Geoelectr.*, 25, 415-435, 1973.
- Coe, R.S., C.S. Grommé, and E.A. Mankinen, Geomagnetic paleointensities from radiocarbon dated lava flows on Hawaii and the question of the Pacific non-dipole low, *J. Geophys. Res.*, 83, 1740-1756, 1978.
- Coe, R.S., C.S. Grommé, and E.A. Mankinen, Geomagnetic paleointensities from excursion sequences in lavas on Oahu, Hawaii, *J. Geophys. Res.*, 89, 1059-1069, 1984.
- Coe, R.S., and M. Prérot, Evidence suggesting extremely rapid field variation during a geomagnetic reversal, *Earth Planet. Sci. Lett.*, 92, 292-298, 1989.
- Courtillot, V., and J. Besse, Magnetic field reversals, polar wander and core-mantle coupling, *Science*, 237, 1140-1147, 1987.

- Dagley, P., and E. Lawley, Paleomagnetic evidence for the transitional behavior of the geomagnetic field, *Geophys. J. R. Astron. Soc.*, **36**, 577-598, 1974.
- Duncan, R.A., Paleosecular variation at the Society islands, French Polynesia, *Geophys. J. R. Astron. Soc.*, **41**, 245-254, 1975.
- Duncan, R. A., and I. McDougall, Linear volcanism in French Polynesia, *J. Volcanol. Geotherm. Res. J.*, 197-227, 1976.
- Fleck, R.J., J.H. Mercer, A.E.M. Nairn, and D.N. Peterson, Chronology of the late Pliocene and early Pleistocene glacial and magnetic events in southern Argentina, *Earth Planet. Sci. Lett.*, **16**, 15-22, 1972.
- Forster J.H., and N. Opdyke, Upper Miocene to recent magnetic stratigraphy in deep-sea sediments, *J. Geophys. Res.*, **75**, 4465-4473, 1970.
- Fuller, M., I. Williams, and K.A. Hoffman, Palaeomagnetic records of geomagnetic field reversals and the morphology of the transitional fields, *Rev. Geophys.*, **17**, 179-203, 1979.
- Gire, C., J.L. Le Mouel, and T. Madden, Motions at the core surface derived from SV data, *Geophys. J. R. Astron. Soc.*, **84**, 1-29, 1986.
- Grommé, S., T.L. Wright, and D.L. Peck, Magnetic properties and oxidation of iron-titanium oxide minerals in Alae and Makapuki lava lakes, Hawaii, *J. Geophys. Res.*, **74**, 5277-5293, 1969.
- Gurarii, G.Z., The Matuyama-Jaramillo geomagnetic inversion in western Turkmenia, *Izv., Earth Phys.*, **17**, 212-218, 1981.
- Gubbins, D., Mechanism for geomagnetic polarity reversals, *Nature*, **326**, 167-169, 1987.
- Gubbins, D., Thermal core-mantle interactions and time-averaged paleomagnetic field, *J. Geophys. Res.*, **93**, 3413-3420, 1988.
- Gubbins, D., and J. Bloxham, Morphology of the geomagnetic field and implications for the geodynamo, *Nature*, **325**, 509-511, 1987.
- Hammond, S.K., S.M. Seylo, and F. Theyer, Geomagnetic polarity transitions in two oriented sediment cores from the Northwest Pacific, *Earth Planet. Sci. Lett.*, **44**, 167-175, 1979.
- Harland, W.B., A.V. Cox, P.G. Llewellyn, C.A.G. Pickton, A.G. Smith, and R. Walters, *A Geologic Time Scale*; Cambridge University Press, New York, 1982.
- Herrero-Bervera, E., and F. Theyer, Non-axisymmetric behavior of Olduvai and Jaramillo polarity transitions recorded in north central Pacific deep-sea sediments, *Nature*, **322**, 159-162, 1986.
- Herrero-Bervera, E., F. Theyer, and C.E. Hesley, Olduvai onset polarity transition: Two detailed paleomagnetic records from the north central Pacific sediments, *Phys. Earth Planet. Inter.*, **49**, 325-342, 1987.
- Hillhouse, J., and A. Cox, Brunhes-Matuyama polarity transition, *Earth Planet. Sci. Lett.*, **29**, 51-64, 1976.
- Hoffman, K.A., Polarity transition records and the geomagnetic dynamo, *Science*, **4296**, 1329-1332, 1977.
- Hoffman, K.A., Behavior of the geodynamo during reversal: a phenomenological model, *Earth Planet. Sci. Lett.*, **44**, 7-17, 1979.
- Hoffman, K.A., Quantitative description of the geomagnetic field during the Matuyama-Brunhes polarity transition, *Phys. Earth Planet. Inter.*, **24**, 229-235, 1981a.
- Hoffman, K.A., Palaeomagnetic excursions, aborted reversals and transitional fields, *Nature*, **294**, 67-69, 1981b.
- Hoffman, K.A., The testing of the geomagnetic reversal models/ recent developments, *Philos. Trans. R. Soc. London, Ser. A*, **306**, 147-159, 1982.
- Hoffman, K.A., A method for the display and analysis of transitional paleomagnetic data, *J. Geophys. Res.*, **89**, 6285-6292, 1984.
- Hoffman, K.A., Transitional field behavior from southern hemisphere lavas: Evidence for two-stage reversals of the geodynamo, *Nature*, **320**, 228-232, 1986.
- Hoffman, K.A., Ancient magnetic reversals: Clues to the geodynamo, *Sci. Am.*, **258**, 76-83, 1988.
- Hoffman, K.A., and M. Fuller, Transitional fields configurations and geomagnetic reversals, *Nature*, **273**, 715-718, 1978.
- Hoffman, K.A., and S.B. Slade, Polarity transition records and the acquisition of remanence: A cautionary note, *Geophys. Res. Lett.*, **13**, 483-486, 1986.
- Karlin, R., and S. Levi, Geochemical and sedimentological control of the magnetic properties of hemipelagic sediments, *J. Geophys. Res.*, **90**, 373-10,392, 1985.
- Karlin, R., M. Lyle, and G.R. Heath, Authigenic magnetite formation in suboxic marine sediments, *Nature*, **326**, 490-493, 1987.
- Kawai, N. T., Sato T. Sueishi, and K. Kobayashi, Paleomagnetic study of deep-sea sediments from the Melanesian basin, *J. Geomagn. Geoelectr.*, **29**, 211-223, 1977.
- Kent, D.V., and D.J. Spariosu, Magnetostratigraphy of Caribbean site 502 hydraulic piston cores, *Initial. Rep. Deep Sea Drill. Proj.*, **68**, 419-433, 1982.
- Khodair, A.A., and R.S. Coe, 1975, Determination of geomagnetic paleointensities in vacuum, *Geophys. J. R. Astron. Soc.*, **42**, 107-115, 1975.
- Kochegura, V.V., and A. Zubakov, Palaeomagnetic time scale of the Ponto-Caspian Plio-Pleistocene deposits, *Palaeogeogr., Palaeoclimatol., Palaeoecol.*, **23**, 151-160, 1978.
- Kono, M., and H. Tanaka, Analysis of the Thellier's method of paleointensity determination, 1, Estimation of statistical errors, *J. Geomagn. Geoelectr.*, **36**, 267-284, 1984.
- Kristjansson, L., Some statistical properties of paleomagnetic directions in Icelandic lava flows, *Geophys. J. R. Astron. Soc.*, **80**, 57-71, 1985.
- Kristjansson, L., and I. Mc Dougall, Some aspects of the late Tertiary geomagnetic field in Iceland, *Geophys. J. R. Astron. Soc.*, **68**, 273-294, 1982.
- Laj, C., S. Guitton, and C. Kissel, Rapid change and near stationary of the geomagnetic field during a polarity reversal, *Nature*, **330**, 145-148, 1987.
- Laj, C., S. Guitton, C. Kissel, and A. Mazaud, Paleomagnetic records of sequential field reversals from the same geographical region at different epoch, *J. Geophys. Res.*, **93**, 11,655-11,666, 1988.
- Lawley, E.H., The intensity of the geomagnetic field in Iceland during Neogene polarity transitions and systematic deviations, *Earth Planet. Sci. Lett.*, **10**, 145-149, 1970.
- Le Mouel, J.L., Outer-core geostrophic flow and secular variation of Earth's geomagnetic field, *Nature*, **311**, 734-735, 1984.
- Levi, S., Comparison of two methods of performing the Thellier experiment (or, how the Thellier method should not be done.), *J. Geomagn. Geoelectr.*, **27**, 245-255, 1975.
- Levi, S., The effect of magnetite particle size on paleointensity determinations of the geomagnetic field, *Phys. Earth Planet. Inter.*, **13**, 245-259, 1977.
- Liddicoat, J.C., Gauss-Matuyama polarity transition, *Philos. Trans. R. Soc. London, Ser. A*, **306**, 121-128, 1982.
- Maenaka, K., Paleomagnetic study of sediments around the Komyoike volcanic ash horizon in Osaka group, Senpoku area, Osaka prefecture, Japan, *Geophys. Res. Lett.*, **6**, 257-260, 1979.
- Mankinen, E.A., J.M. Donnelly, and C.S. Grommé, Geomagnetic polarity event recorded and 1.1 Ma BP on Cobb Mountain, Clear Lake volcanic field, California, *Geology*, **6**, 653-656, 1978.
- Mankinen, E.A., and G.B. Dalrymple, Revised geomagnetic polarity time scale for the interval 0-5 Ma B.P., *J. Geophys. Res.*, **84**, 615-626, 1979.
- Mankinen, E.A., J.M. Donnelly-Nolan, C.S. Grommé, and B.C. Hearn JR, Paleomagnetism of the Clear Lake volcanics and new limits of the age of the Jaramillo normal polarity event, *U.S. Geol. Surv. Prof. Pap.*, **1141**, 67-82, 1981.
- Mankinen, E.A., and C.S. Grommé, Paleomagnetic data from the Coso Range, California and the current status of the Cobb Mountain normal geomagnetic event, *Geophys. Res. Lett.*, **9**, 1279-1282, 1982.
- Mankinen, E.A., M. Prévot, C.S. Grommé, and R.S. Coe, The Steens Mountain (Oregon) geomagnetic polarity transition. 1- Directional history, duration of episodes and rock magnetism, *J. Geophys. Res.*, **90**, 10,393-10,416, 1985.
- McDougall, I., and F.H. Chamalaun, Geomagnetic polarity scale of time, *Nature*, **212**, 1415-1418, 1966.
- McElhinny, M.W., and R.T. Merrill, Geomagnetic secular variation over the past 5 Ma, *Rev. Geophys.*, **13**, 687-708, 1975.
- McFadden, P.L., and M.W. McElhinny, A physical model for paleosecular variation, *Geophys. J. R. Astron. Soc.*, **78**, 809-830, 1984.
- McFadden, P.L., and R.T. Merrill, Lower mantle convection and geomagnetism, *J. Geophys. Res.*, **89**, 3354-3362, 1984.
- McFadden, P.L., and R.T. Merrill, Geodynamo energy source constraints from paleomagnetic data, *Phys. Earth Planet. Inter.*, **43**, 22-33, 1986.
- McFadden, P.L., R.T. Merrill, and M.W. McElhinny, Dipole/Quadrupole family modeling of paleosecular variation, *J. Geophys. Res.*, **93**, 11,583-11,588, 1988.
- Merrill, R.T., and P.L. McFadden, Secular variation and the origin of geomagnetic field reversals, *J. Geophys. Res.*, **93**, 11,589-11,598, 1988.
- Nagata, T., Y. Arai, and K. Momose, Secular variation of the Geomagnetic total force during the last 5000 years, *J. Geophys. Res.*, **68**, 5277-5282, 1963.

- Niitsuma, N.D., Paleomagnetic and paleoenvironmental study of sediments recording Matuyama-Brunhes geomagnetic reversal, *Tohoku Univ. Sci. Rep. Geol.*, 43, 1-39, 1971.
- Ninkovich, D., N. Opdyke, B.C. Heezen, and J.H. Foster, Paleomagnetic stratigraphy, rates of deposition and tephrochronology in north Pacific deep-sea sediments, *Earth Planet. Sci. Lett.*, 1, 476-492, 1966.
- Olson, P., Geomagnetic polarity reversals in a turbulent core, *Phys. Earth Planet. Inter.*, 33, 260-274, 1983.
- Opdyke, N.D., D.V. Kent, and W. Lowrie, Details of magnetic polarity transitions recorded in high deposition rate, deep-sea core, *Earth Planet. Sci. Lett.*, 20, 315-324, 1973.
- Prévot, M., E.A. Mankinen, S. Grommé, and A. Lecaille, High paleointensities of the geomagnetic field from thermomagnetic studies on rift valley pillow basalts from the mid-Atlantic ridge., *J. Geophys. Res.*, 88, 2316-2326, 1983.
- Prévot, M., E.A. Mankinen, C.S. Grommé, and R.S. Coe, How the geomagnetic field vector reverse polarity, *Nature*, 316, 230-234, 1985a.
- Prévot, M., E.A. Mankinen, R.S. Coe, and C.S. Grommé, The steens Mountain geomagnetic polarity transition 2. Field intensity variation and discussion of reversal models, *J. Geophys. Res.*, 90, 10417-10448, 1985b.
- Rea, D.K., and R.J. Blakely, Short-wavelength magnetic anomalies in a region of rapid seafloor spreading, *Nature*, 255, 126-128, 1975.
- Roperch, P., Comportement du champ magnétique terrestre au cours de transitions de polarité, Thèse, *Trav. et Doc. ORSTOM, TDM 26*, 209 pp., 1987.
- Roperch, P., and A. Chauvin, Transitional geomagnetic field behavior: Volcanic records from French Polynesia, *Geophys. Res. Lett.*, 14, 151-154., 1987.
- Roperch, P., and R.A. Duncan, Records of geomagnetic reversals from volcanic islands of French polynesia, 1, Paleomagnetic study of a polarity transition recorded on a lava sequence from the island of Huahine., *J. Geophys. Res.*, this issue.
- Senanayake, W.E., M.W. McElhinny, and P.L. Mc Fadden, Comparison between the Thellier's and Shaw's paleointensity methods using basalts less than 5 million years old, *J. Geomagn. Geoelectr.*, 34, 141-161, 1982.
- Shaw, J., Strong geomagnetic fields during a single Icelandic polarity transition, *Geophys. J. R. Astron. Soc.*, 40, 345-350, 1975.
- Shaw, J., Further evidence for a strong intermediate state of the paleomagnetic field, *Geophys. J. R. Astron. Soc.*, 48, 263-269, 1977.
- Sigurgeirsson, T., Directions of magnetization in Icelandic basalts, *Adv. Phys.*, 6, 240-246, 1957.
- Sueishi, T., T. Sato, N. Kawai and K. Kobayashi, Short geomagnetic episode in the Matuyama Epoch, *Phys. Earth Planet. Inter.*, 19, 1-11, 1979.
- Thellier, E., and O. Thellier, Sur l'intensité du champ magnétique terrestre dans le passé historique et géologique, *Ann. Geophys.*, 15, 285-376, 1959.
- Theyer, F., E. Herrero-Bervera, and V. Hsu, The zonal harmonic model of polarity transitions/ a test using successive reversals, *J. Geophys. Res.*, 90, 1963-1982, 1985.
- Valet, J.P., Inversions géomagnétiques du Miocene supérieur en Crete. Modalités de renversement et caractéristiques du champ de transition, thèse, 195 pp., Univ. d'Orsay, France, 1985.
- Valet, J.P., and C. Laj, Invariant and changing transitional field configurations in a sequence of geomagnetic reversals, *Nature*, 311, 552-555, 1984.
- Valet, J.P., L. Tauxe, and D.R. Clark, The Matuyama-Brunhes transition recorded from the lake Tecopa sediments (California), *Earth Planet. Sci. Lett.*, 87, 463-472, 1988a.
- Valet, J.P., C. Laj, and C.G. Langereis, Sequential geomagnetic reversals recorded in Upper Tortonian marine clays in western Crete (Greece), *J. Geophys. Res.*, 93, 1131-1151, 1988b.
- Valet, J.P., L. Tauxe, and B. Clement, Equatorial and mid-latitude records of the last geomagnetic reversal from the Atlantic Ocean, *Earth Planet. Sci. Lett.*, 94, 371-384, 1989.
- Van Zijl, J.S.V., K.W.T. Graham, and A.L. Hales, The paleomagnetism of the Stormberg Lavas of South Africa, 1, Evidence for a genuine reversal of the earth's field in Triassic-Jurassic Times., *Geophys. J. R. Astron. Soc.*, 7, 169-182, 1962.
- Watkins, N.D., Short period geomagnetic events in deep-sea sedimentary cores, *Earth Planet. Sci. Lett.*, 4, 341-349, 1968.
- Watkins, N.D., and A. Abdel-Monem, detection of the Gilsa geomagnetic polarity event on the island of Madeira, *Geol. Soc. Am. Bull.*, 82, 191-198, 1971.
- Weeks, R.J., M. Fuller, and I. Williams, The effects of recording medium upon reversal records, *Geophys. Res. Lett.*, 15, 1255-1258, 1988.
- Williams, I., and M. Fuller, Zonal harmonic models of reversal transition fields, *J. Geophys. Res.*, 86, 11657-11665, 1981.
- Williams, I., R. Weeks, and M. Fuller, A model for transition field during geomagnetic reversals, *Nature*, 332, 719-720, 1988.
- Wilson, R.L., P. Dagle, and A.G. McCormack, Paleomagnetic evidence about the source of the geomagnetic field, *Geophys. J. R. Astron. Soc.*, 28, 213-224, 1972.

A. Chauvin and P. Roperch, ORSTOM et Laboratoire de Géophysique Interne, Université de Rennes I, av. Général Leclerc, 35042 Rennes France.

R.A. Duncan, College of Oceanography, Oregon State University Corvallis, OR97331.

(Received March 10, 1989;
revised October 3, 1989;
accepted November 7, 1989.)